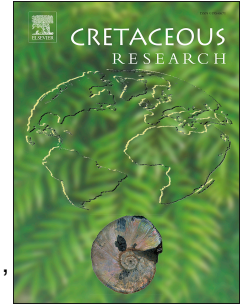


Journal Pre-proof

Testing the persistence of Carcharodontosauridae (THEROPODA) in the upper cretaceous of Patagonia based on dental evidence

J.G. Meso, R.D. Juárez Valieri, J.D. Porfiri, S.A.S. Correa, A.G. Martinelli, G.A. Casal, J.I. Canudo, F. Poblete, D. Dos Santos



PII: S0195-6671(21)00122-1

DOI: <https://doi.org/10.1016/j.cretres.2021.104875>

Reference: YCRES 104875

To appear in: *Cretaceous Research*

Received Date: 6 September 2020

Revised Date: 14 March 2021

Accepted Date: 22 April 2021

Please cite this article as: Meso, J.G., Juárez Valieri, R.D, Porfiri, J.D., Correa, S.A.S., Martinelli, A.G., Casal, G.A., Canudo, J.I., Poblete, F., Dos Santos, D., Testing the persistence of Carcharodontosauridae (THEROPODA) in the upper cretaceous of Patagonia based on dental evidence, *Cretaceous Research*, <https://doi.org/10.1016/j.cretres.2021.104875>.

This is a PDF file of an article that has undergone enhancements after acceptance, such as the addition of a cover page and metadata, and formatting for readability, but it is not yet the definitive version of record. This version will undergo additional copyediting, typesetting and review before it is published in its final form, but we are providing this version to give early visibility of the article. Please note that, during the production process, errors may be discovered which could affect the content, and all legal disclaimers that apply to the journal pertain.

© 2021 Elsevier Ltd. All rights reserved.

Credit Author Statement

Jorge Gustavo Meso: Writing - Original Draft, Figures, Writing - Review & Editing

Ruben Juárez Valieri: Writing - Original Draft, Writing - Review & Editing

Juan Porfiri: Writing - Original Draft, Writing - Review & Editing

Samuel Correa: Writing - Original Draft, Figures, Writing - Review & Editing

Agustin Martinelli: Writing - Original Draft, Writing - Review & Editing

Gabriel Casal: Writing - Original Draft

Juan Ignacio Canudo: Writing - Original Draft

Federico Poblete: Writing - Original Draft

Domenica Dos Santos: Writing - Original Draft

1 **TESTING THE PERSISTENCE OF CARCHARODONTOSAURIDAE**
2 **(THEROPODA) IN THE UPPER CRETACEOUS OF PATAGONIA BASED ON**
3 **DENTAL EVIDENCE**

4

5 J.G. MESO^{1,2}, R.D JUÁREZ VALIERI³, J.D. PORFIRI^{4,5,6}, S.A.S. CORREA^{1,2}, A.G.
6 MARTINELLI⁷, G.A. CASAL⁸, J.I. CANUDO⁹, F. POBLETE⁴, and D. DOS
7 SANTOS^{4,5,6}

8

9 ¹Universidad Nacional de Río Negro. Instituto de Investigación en Paleobiología y
10 Geología. Río Negro. Argentina.

11 ²IIPG. UNRN. Consejo Nacional de Investigaciones científicas y Tecnológicas
12 (CONICET). Av. Roca 1242, (R8332EXZ) General Roca, Río Negro, Argentina.
13 jgmeso@unrn.edu.ar ORCID ID: <https://orcid.org/0000-0002-5522-8569>

14 ³Secretaría de Cultura de la Provincia de Río Negro, Museo Provincial Carlos
15 Ameghino, Belgrano 2150, 8324 Cipolletti, Río Negro, Argentina.
16 rubendjuarez@gmail.com

17 ⁴Museo del Desierto Patagónico, calle 6 S/N, 8305 Añelo, Neuquén, Argentina.

18 ⁵Museo de Ciencias Naturales. Universidad Nacional del Comahue. Buenos Aires 1400
19 (8300), Neuquén, Neuquén, Argentina. juan.porfiri@central.uncoma.edu.ar,
20 domenica.santos@central.uncoma.edu.ar

21 ⁶Cátedra de Reptiles Mesozoicos. Facultad de Ingeniería. Universidad Nacional del
22 Comahue. Buenos Aires 1400 (8300), Neuquén, Neuquén, Argentina.

23 ⁷Sección Paleontología de Vertebrados, CONICET–Museo Argentino de Ciencias
24 Naturales ‘Bernardino Rivadavia’, Avenida Ángel Gallardo 470, C1405DJR CABA,
25 Argentina. agustin_martinelli@yahoo.com.ar ORCID ID: [https://orcid.org/0000-0003-](https://orcid.org/0000-0003-4489-0888)
26 4489-0888

27 ⁸Laboratorio de Paleontología de Vertebrados, Facultad de Ciencias Naturales y
28 Ciencias de la Salud, Universidad Nacional de la Patagonia San Juan Bosco, Ruta
29 provincial N°1, Km. 4, Comodoro Rivadavia, Chubut, Argentina.

30 ⁹Grupo Aragosaurus-IUCA, Paleontología, Facultad de Ciencias, Universidad de
31 Zaragoza, C/Pedro Cerbuna, 12, 50009 Zaragoza, Spain. jicanudo@unizar.es

32

33

34

35 **Abstract**

36 The deposits corresponding to the Upper Cretaceous Neuquén and San Jorge Gulf
37 basins from northern and central Patagonia have provided two of the most complete
38 sequences of terrestrial vertebrate faunas of all Gondwanan landmasses. Among the
39 carnivorous components, the carcharodontosaurid theropods appeared as common
40 elements during the Early Cretaceous and the earliest Late Cretaceous in northern and
41 central Patagonia. Although recorded mostly in the lower Turonian, isolated teeth
42 suggest their presence in younger strata in northern and central Patagonia, reaching the
43 clade in the region as late as the early Maastrichtian. Here, we verify the assignment of
44 such isolated teeth previously identified as belonging to Carcharodontosauridae from
45 the Upper Cretaceous strata of northern and central Patagonia. Using three different

46 methods, namely a cladistic analysis performed on a dentition-based data matrix, and
47 discriminant and cluster analyses conducted on a large dataset of theropod crown
48 measurements, we assign a tooth from Candeleros Formation to carcharodontosaurid
49 theropods and teeth from Cerro Lisandro, Bajo Barreal, Portezuelo, Plottier and Allen
50 formations to abelisaurid theropods. These new reappraisals provide additional evidence
51 about the extinction of Carcharodontosauridae in South America at about the late
52 Turonian–earliest Coniacian as part of a general faunistic turnover event, with the last
53 clear evidence of this lineage in Patagonia coming from the early–middle Turonian.

54 **Keywords.** Shed teeth, taxonomic identification, Late Cretaceous, Patagonia, South
55 America, Carcharodontosauridae.

56

57 **1. Introduction**

58 Carcharodontosauridae is a clade of medium to large sized cretaceous theropod
59 dinosaurs, with a wide paleogeographic distribution. They are present in both Laurasian
60 (Asia, Europe and North America) and western Gondwanan landmasses (Africa and
61 South America) (Brusatte *et al.*, 2009; Novas *et al.*, 2013; Csiki-Sava *et al.*, 2016;
62 Cuesta *et al.*, 2018a, b). The clade represents an important radiation within allosauroid
63 theropods that ranged from the Late Jurassic to the mid-Cretaceous (Brusatte and
64 Sereno, 2008; Rauhut, 2011). Although the monophyly of Carcharodontosauridae is
65 widely accepted, its phylogenetic relationships amongst other theropods, are far to be
66 conclusive (Benson *et al.*, 2010; Carrano *et al.*, 2012; Porfiri *et al.*, 2014; Apesteguía *et*
67 *al.*, 2016), as are their internal relationships (Brusatte and Sereno, 2008; Novas *et al.*,
68 2013; Canale *et al.*, 2014; Cuesta *et al.*, 2018a,b).

69 At present, the South American record of Carcharodontosauridae, which comes
70 entirely from Argentine Patagonia, is undisputedly from the Lower to lower Upper
71 Cretaceous; however, previous identifications of fragmentary materials carry their
72 biochron to the Maastrichtian (e.g., Martinelli and Forasiepi, 2004). The record includes
73 the basal *Lajasvenator ascheriae* from the Valanginian Mulichinco Formation (Coria *et*
74 *al.*, 2020); the highly derived *Tyrannotitan chubutensis* from the Aptian Cerro Barcino
75 Formation (Novas *et al.*, 2005); *Giganotosaurus carolinii* from the lower Cenomanian
76 Candeleros Formation (Coria and Salgado, 1995); and *Mapusaurus roseae* and
77 *Taurovenator violentei* from the upper Cenomanian to lower Turonian Huincul
78 Formation (Coria and Currie, 2006; Motta *et al.*, 2016). These last two taxa have been
79 recently proposed as likely synonyms (Coria *et al.*, 2020: p. 18).

80 In addition to these nominated taxa, several isolated teeth from Argentina have
81 been considered as belonging to Carcharodontosauridae. Examples include teeth coming
82 from the middle Turonian Cerro Lisandro Formation (Salgado *et al.*, 2009), upper
83 Turonian to lower Coniacian Portezuelo Formation (Calvo and Veralli, 2004), and the
84 upper Campanian to lower Maastrichtian Allen Formation (Martinelli and Forasiepi,
85 2004). These latter records together with very fragmentary cranial material and isolated
86 teeth from the Bauru Group in southeastern Brazil (see Delcourt *et al.*, 2020), were
87 utilized as evidence of a long persistence of the clade in South America. The assignation
88 of some of these Patagonian teeth to Carcharodontosauridae has been previously
89 questioned by their resemblance to some abelisaurid teeth (*i.e.*, Canale *et al.*, 2009) or
90 by the distributions of features previously considered as diagnostic of
91 Carcharodontosauridae (*i.e.*, Brusatte *et al.*, 2007).

92 The aim of this contribution is to describe and analyze, with qualitative and
93 quantitative techniques, the systematic of isolated teeth from Patagonia originally

94 considered as belonging to Carcharodontosauridae from the middle Turonian to lower
95 Maastrichtian. We also include an undescribed shed tooth from the Candeleros
96 Formation. With this review we seek to evaluate the persistence of the clade in southern
97 South America later than the confirmed occurrence of the Carcharodontosauridae in the
98 middle Turonian.

99

100 **1.1. Institutional Abbreviations.** **AMNH FARB**, American Museum of Natural History
101 (fossil amphibian reptiles and bird specimens), New York, USA; **AODF**, Australian
102 Age of Dinosaurs Fossil, Winton, Queensland, Australia; **BP**, Evolutionary Studies
103 Institute (formerly “Bernard Price Institute for Palaeontological Research”), University
104 of the Witwatersrand, Johannesburg, South Africa; **DGM**, Museu de Ciências da Terra,
105 Rio de Janeiro, Brazil; **ENDEMAS-Pv**, Ente de Desarrollo para la Margen Sur,
106 Paleontología de Vertebrados, Cipolletti, Argentina **FMNH PR**, Field Museum of
107 Natural History, Chicago, USA; **FPDM-V**, Fukui Prefectural Dinosaur Museum,
108 Muroko, Terao, Katsuyama, Fukui, Japan; **GSI-IM**, Geological Survey of India, Indian
109 Museum, Kolkata, India; **GZG**, Geowissenschaftliches Zentrum der Universität
110 Göttingen, Göttingen, Germany; **ISIR**, Indian Statistical Institute, Reptiles, Kolkata,
111 India; **IVPP**, Institute for Vertebrate Paleontology and Paleoanthropology, Beijing,
112 China; **MACN-Pv-RN**, Museo Argentino de Ciencias Naturales “Bernardino
113 Rivadavia”, Colección Paleontología de Vertebrados (Pv), Colección Provincia de Río
114 Negro (RN), Buenos Aires, Argentina; **MAU-Pv-LI**, Museo Municipal “Argentino
115 Urquiza”, Rincón de los Sauces, Argentina; **MCNA**, Museo de Ciencias Naturales y
116 Antropológicas “Juan Cornelio Moyano”, Mendoza, Argentina; **MCF-PVPH**, Museo
117 Municipal “Carmen Funes”, Paleontología de Vertebrados, Plaza Huincul, Argentina;
118 **MDPA-Pv**, Museo del Desierto Patagónico, Añelo, Argentina; **MGUP**, Museo di

119 Geologia e Paleontologia, Università di Palermo, Italy; **MHNA-PV**, Muséum d'Histoire
120 Naturelle d'Aix-en-Provence, France; **MIWG**, Dinosaur Isle, Isle of Wight Museum
121 Services, Sandown, UK; **MLP**, Museo de La Plata, La Plata, Argentina; **MMCH-PV**,
122 Museo Municipal "Ernesto Bachmann", Villa El Chocón, Argentina; **MNHN**, Muséum
123 national d'Histoire naturelle, Paris, France; **MNN**, Musée National du Niger, Niamey,
124 Niger; **MPCA**, Museo Provincial "Carlos Ameghino", Cipolletti, Argentina; **MPCM**,
125 Museo Paleontológico Cittadino di Monfalcone, Gorizia, Italy; **MPCN**, Museo
126 Patagónico de Ciencias Naturales "Juan Carlos Salgado", General Roca, Argentina;
127 **MPM-Pv**, Museo "Padre Molina", Paleontología de Vertebrados, Río Gallegos,
128 Argentina; **MPUR**, Museo di Paleontologia of the Sapienza Università di Roma, Rome,
129 Italy; **MUCPv**, Museo de Ciencias Naturales de la Universidad Nacional de Comahue,
130 Paleontología de Vertebrados, Neuquén, Argentina; **NHFO**, Natural History Fossil
131 Collection, Qatar Museum Authority, Doha, Qatar; **NHMUK**, The Natural History
132 Museum, Palaeontology Vertebrates, London, United Kingdom; **NMB**,
133 Naturhistorisches Museum Braunschweig, Braunschweig, Germany; **OCP**, Office
134 Chérifien des Phosphates, Khouribga, Morocco; **PVL**, Fundación 'Miguel Lillo,' San
135 Miguel de Tucumán, Argentina; **PVSJ**, Museo de Ciencias Naturales, Universidad
136 Nacional de San Juan, San Juan, Argentina; **RTMP**, Royal Tyrrell Museum of
137 Palaeontology, Drumheller, Canada; **SMA**, Sauriermuseum Aathal, Aathal,
138 Switzerland; **UA**, Université d'Antananarivo, Antananarivo, Madagascar; **UCMP**,
139 University of California Museum of Paleontology, Berkeley, USA; **UNPSJB-PV**,
140 Universidad Nacional de la Patagonia San Juan Bosco, Paleontología de Vertebrados,
141 Comodoro Rivadavia, Argentina; **USNM**, United States National Museum,
142 Washington, USA; **YPM**, Yale Peabody Museum of Natural History, Yale, USA;
143 **WDC-CCPM**, Wyoming Dinosaur Center, Thermopolis, USA.

144

145 **1.2. Anatomical abbreviations.** **AL**, apical length; **CA**, crown angle; **CBL**, crown base;
146 **CBR**, crown base ratio; **CBW**, crown base width; **CH**, crown height; **CHR**, crown
147 height ratio; **CTU**, crown transverse undulation density; **DA**, distoapical denticle
148 density; **DAVG**, average distal denticle density; **DB**, distobasal denticle density; **DC**,
149 distocentral denticle density; **DDT**, dentine thickness distally; **DLAT**, dentine thickness
150 labially; **DLIT**, dentine thickness lingually; **DMT**, dentine thickness mesially; **DSDI**,
151 denticle size density index; **FABL**, fore-aft basal length; **LAF**, number of flutes on the
152 labial surface of a crown; **LIF**, number of flutes on the lingual surface of a crown; **MA**,
153 mesioapical denticle density; **MAVG**, average mesial denticle density; **MB**, mesio-
154 basal denticle density; **MC**, mesiocentral denticle density; **MCE**, mesial carina extent;
155 **MCL**, mid crown length; **MCR**, mid-crown ratio; **MCW**, mid-crown width; **MDE**,
156 mesiobasal denticles extent.

157

158 **2. Material and Methods.**

159 **2.1. Materials included in the present study**

160 The analysis presented here is based on datasets published by Hendrickx *et al.* (2020).
161 Additionally, we include nine new specimens from different stratigraphic units of
162 Patagonia, namely the Neuquén and San Jorge Gulf basins. The specimens incorporated
163 in the current study are listed in Table 1. This table includes the stratigraphic
164 provenance and previous assignments of the material referred to Carcharodontosauridae.

165 **2.2. Comparative methodology and terminology.** For the studied teeth, we measured
166 eleven variables (i.e., CBL, CBW, CH, AL, MCL, MCW, CTU, MA, MC, DC, DA;

167 Table 1) with a digital caliper of 150 mm (6"), with an accuracy of 0.01 mm. Each tooth
168 was described using the dental nomenclature and protocol proposed by Hendrickx *et al.*
169 (2015a) and then compared to the dentition of 155 non-avian theropod species-level
170 taxa (Young *et al.*, 2019; Hendrickx *et al.*, 2020). We used a binocular loupe to observe
171 denticles, crown ornamentations and enamel surface texture.

172 The terminology concerning anatomical orientation follows the recommendation
173 of Smith and Dodson (2003) and Hendrickx *et al.* (2015a). For the morphometric and
174 anatomical terms and abbreviations, we follow Smith *et al.* (2005) and Hendrickx *et al.*
175 (2015a). Similarly, we follow/adopt phylogenetic definitions by Hendrickx *et al.*
176 (2015a, 2020).

177 **2.3. Cladistic analysis.** With the objective to explore their phylogenetic affinities, dental
178 material was first explored by performing a cladistic analysis on an updated version of
179 the data matrix created by Hendrickx and Mateus (2014), which focus on the dentition
180 of non-avian theropods. The most updated version of this data matrix was published by
181 Hendrickx *et al.* (2020) and includes 146 dental characters scored across 105 theropod
182 genera. We recognized six dental morphotypes among the sample of theropod teeth
183 (Table 1), which we scored as separated operational taxonomic units (OTUs).

184 We followed the methodology by Young *et al.* (2019) and Hendrickx *et al.*
185 (2020) and conducted the cladistic analysis with TNT 1.1 (Goloboff *et al.* 2008) using a
186 backbone tree topology and the positive constraint command, setting the three dental
187 morphotypes as floating terminals (supplementary information 1.2). As in Young *et al.*
188 (2019) and Hendrickx *et al.* (2020), the topological tree was built based on the results of
189 the phylogenetic analyses of Müller *et al.* (2018) for non-neotheropod saurischians,
190 Ezcurra (2017) for non-averostran neotheropods, Rauhut and Carrano (2016) and Wang

191 *et al.* (2017) for Ceratosauria, Carrano *et al.* (2012) and Rauhut *et al.* (2012, 2016) for
192 non-coelurosaurian tetanurans, Brusatte and Carr (2016) for Tyrannosauroida, and Cau
193 *et al.* (2017) for other coelurosaurs. As the search strategy, we used a combination of
194 the tree-search algorithms Wagner trees, TBR branch swapping, sectorial searches,
195 Ratchet (perturbation phase stopped after 20 substitutions) and Tree Fusing (5 rounds)
196 until 100 hits of the same minimum tree length were reached. Then, the trees were
197 subjected to a final round of TBR branch swapping (Hendrickx *et al.*, 2020: p. 4). We
198 also performed two additional cladistic analyses as did Young *et al.*'s (2019) and
199 Hendrickx *et al.*'s (2020). One analysis used the dentition-based dataset without
200 constraints, and the second one used a data matrix restricted to crown-based characters
201 (Hendrickx *et al.*, 2020: p. 11).

202 **2.4. Discriminant analysis.** We included each of the nine shed teeth of theropods to
203 classify them and predict their optimal classifications inside 'family-level' groupings
204 based on quantitative data, performing a discriminant function analysis (DFA) on the
205 dataset of theropod crown measurements published by Hendrickx *et al.* (2020). This
206 dataset includes fifteen measurements (i.e., CBL, CBW, CH, AL, CBR, CHR, MCL,
207 MCW, MCR, MSL, LAF, LIF, CA, MDL, DCL) taken in 1335 teeth belonging to 89
208 taxa (84 species and five indeterminate family-based taxa) separated into 20
209 monophyletic or paraphyletic groups. Because many researchers measure dinosaur
210 crowns differently (Hendrickx *et al.*, 2020), a second analysis was conducted on a
211 dataset restricted to measurements taken by Christophe Hendrickx (see Hendrickx *et al.*,
212 2020). Finally, given that most of the isolated theropod teeth under study belonged to
213 relatively large sized animals, a third analysis was performed on a dataset restricted to
214 theropod taxa with crowns of more than 20 mm. These two datasets include 725 and

215 400 teeth belonging to 53 and 46 theropod taxa each separated into 13 groups,
216 respectively.

217 The discriminant function analysis was performed following the protocol
218 detailed by Young *et al.* (2019), in which, all variables were log-transformed to
219 normalize the quantitative variables. The DFA was run in Past 3 version 3.19 (Hammer
220 *et al.* 2001) using the Discriminant analysis (LDA) function. Each tooth included in the
221 present study (Table 1) was treated as the unknown taxon so that they could be
222 classified at genus and group level in each analysis.

223

224 **2.5. Cluster analysis.** A cluster analysis was performed in Past3 on the different
225 datasets using the Paired group algorithm and a Neighbour joining clustering; we chose
226 Euclidean distances for the Similarity Index (see Young *et al.*, 2019; Hendrickx *et al.*,
227 2020).

228

229 **4. Systematic Paleontology**

230 **4.1. Candeleros Formation**

231 **Theropoda** Marsh, 1881

232 **Tetanurae** Gauthier, 1986

233 **Allosauroidea** Currie and Zhao, 1993

234 **Carcharodontosauridae** Stromer, 1931

235 **Gen. and sp. indet.**

236

237 **Material.** MDPA-Pv 005 (Figure 3).

238 **Locality and Horizon.** Aguada Pichana area (38°20'30"S; 69°10'4"W), located in the
239 center of Neuquén province, Argentina; upper section of the Candeleros Formation,
240 lower Cenomanian, Upper Cretaceous (Garrido, 2010).

241 **State of preservation and general morphology.** The tooth is almost complete with most
242 of the crown preserved (i.e., interpreted here as a shed tooth). MDPA-Pv 005 is quite
243 damaged, with the labial surface highly eroded while the lingual side is less damaged.
244 Nevertheless, the enamel of the crown is well observable in many parts of both faces.
245 Additionally, a horizontal fracture of post-mortem type is observed in the middle of the
246 crown, which attributed to the fall of the tooth and/or to processes that occurred later.
247 Likewise, the tooth lacks its tip and most basal sector (i.e., sector of the cervix). The
248 denticles are much worn both in the mesial and the distal carinae, although very few of
249 them show their original shape.

250 **Crown overall morphology.** Due to its labiolingually compressed crown with a distal
251 curvature, and serrated carinae, this element is considered as ziphodont type. While it is
252 not possible to calculate the exact value of the labiolingual compression of the crown
253 (CBR), said ratio is considered to be important to normal. This quantification is based
254 on the preserved proportions of the crown where the ratio is equal to 0.48. Given that
255 the missing basal sector is negligible, it is possible to infer that this value should be
256 close to 0.5. A similar inference can be done regarding baso-apical elongation of the
257 crown. Thus, based on parameters provided by Hendrickx and Mateus (2014), this ratio
258 is normal (CHR=2.2).

259 In apico-basal sense the mesial margin of the crown is strongly convex in lateral
260 view with a serrated carina. The distal margin of the crown is slightly concave in lateral

261 view, also presenting a serrated carina. Although both labial and lingual surfaces are
262 mesiodistally convex in apical view, the lingual surface is concave in apico-basal
263 orientation. In basal view, both lingual and labial surfaces are strongly convex, and their
264 faces converge mesially and distally in conspicuous carinae.

265 The cross-section is lenticular at near the level of the cervix, while on apical
266 view its cross-section is parlinon-shaped. In the mesial view, the mesial carina is
267 diagonally oriented to the labial face, and although its basalmost portion is missing, it
268 must have extended to the cervix or just above it based on the size of denticles observed
269 on the basalmost region. In the distal view, the distal margin is centrally positioned and
270 appears to be lingually displaced weakly. On each side of both faces there is a concave
271 surface adjacent to the distal carina.

272 **Denticles.** The mesial carina bears 10 denticles per 5 mm at mid-crown, and 15
273 denticles per 5 mm close to the apex. The distal carina possesses 15 denticles per 5 mm
274 at mid-crown and 17 denticles per 5 mm at its base. However, the density of denticles
275 close to the cervix is unknown since the carina is eroded and damaged. Similarly, the
276 apical distal denticles density could not be calculated because this margin is highly
277 eroded. In both carinae, denticle densities increase apically and basally from mid-height
278 (DSDI = 1.5). Although in several portions of both carinae the denticles are partially
279 eroded, both mesial and distal denticles are symmetrical to slightly asymmetrically
280 convex with a biconvex external margin. The interdenticular space is narrow, less than
281 one-third of the denticles width.

282 **Crown surface and ornamentation.** The crown of the tooth possesses arcuate marginal
283 undulations on both surfaces about the distal margin. These are well compacted,
284 abundant and horizontally oriented in mesial sense. Transverse undulations, flutes,

285 longitudinal grooves, or ridges are absent. The enamel texture is braided (i.e., oriented
286 enamel texture in alternating with interweaving grooves and sinuous ridges *sensu*
287 Hendrickx *et al.*, 2015).

288

289 **4.2. Cerro Lisandro Formation**

290 **Theropoda** Marsh, 1881

291 **Ceratosauria** Marsh, 1884

292 **Abelisauroidea** Bonaparte, 1991

293 **Abelisauridae** Bonaparte and Novas, 1995

294 **Gen. and sp. indet.**

295

296 **Material.** Endemas-Pv 2 (Figure 4).

297 **Locality and Horizon.** El Anfiteatro area, la Bajada Sector (39°17'44"S; 68°27'33"W),
298 located at the center-west of the Río Negro province, Argentina; upper section of the
299 Cerro Lisandro Formation, middle to upper Turonian, Upper Cretaceous (Salgado *et al.*,
300 2009; Garrido, 2010).

301 **State of preservation and general morphology.** Endemas-Pv 2 is an almost complete
302 tooth that lacks a very basal sector of the crown. Some denticles are worn out, although
303 it is possible to observe the density along both carinae. A horizontal fracture of type
304 post-mortem (i.e., attributed to the fall of the tooth and/or to processes that occurred
305 later) located in the close to the apex of the crown is observable.

306 **Crown overall morphology.** The tooth is interpreted as a mesial tooth of the series. The
307 preserved height is 31.75 mm, the labiolingual compression of the crown (CBR) is
308 equal to 0.77, and the baso-apical elongation of the crown (CHR) is 2.35. In lateral
309 view, the mesial and distal margins are strongly convex baso-apically with the apex
310 positioned centrally on the crown. In both carinae, the denticles are well developed.
311 Both in apical and basal views, the lingual and labial surfaces are strongly convex and
312 their faces converge mesially and distally in well visible carinae. In cross-section almost
313 at the level of the cervix, the tooth is salinon-shaped. The mesial and distal carinae are
314 strongly displaced lingually. On each side of both faces there is a concave surface
315 adjacent to the distal carina, as there is a lingual surface adjacent to the mesial carina.

316 **Denticles.** The mesial carina bears 12 denticles per 5 mm at mid-crown and close to the
317 apex, whereas it possesses 13 denticles per 5 mm close to the cervix. The distal carina
318 bears 11 denticles per 5 mm at mid-crown and close to the apex, and possesses 13
319 denticles per 5 mm close to the cervix. The denticles are rectangular, chisel-like and
320 slightly inclined apically (Salgado *et al.*, 2009). The interdenticular space is narrow, less
321 than one-third of the denticles width.

322 **Crown surface and ornamentation.** The crown of the tooth possesses arcuate marginal
323 undulations on both surfaces about the distal margin. These are well compacted,
324 abundant and horizontally oriented in mesial sense. Transverse undulations, flutes,
325 longitudinal grooves, or ridges are absent. The enamel texture is smooth.

326

327 **4.3. Bajo Barreal Formation**

328 **Theropoda** Marsh, 1881

329 **Ceratosauria** Marsh, 1884

330 **Abelisauroidea** Bonaparte, 1991

331 **Abelisauridae** Bonaparte and Novas, 1995

332 **Gen. and sp. indet.**

333 **Material.** UNPSJB-PV 969 (Figure 5).

334 **Locality and Horizon.** Western flank of Sierra de San Bernardo area, Estancia Ocho
335 Hermanos locality (45°17'37"S; 69°35'29"W), located at the center-south of the Chubut
336 province, Argentina; uppermost levels of the Lower Member of the Bajo Barreal
337 Formation, lower Cenomanian to upper Turonian, Upper Cretaceous (Casal *et al.*, 2009,
338 2016).

339 **State of preservation and general morphology.** The tooth consists of a fragment of
340 crown with well-preserved labial and lingual surfaces and including the enamel layer. It
341 lacks its most apical apex, whereas the most basal sector of the crown is strongly eroded
342 at level of the cervix. The mesial carina is well-preserved, although lacks the apical tip.
343 The distal carina lacks its basal and apical sectors. In both carinae, the denticles are well
344 preserved and show their original shape.

345 **Crown overall morphology.** The shed tooth from Bajo Barreal Formation described
346 originally by Casal *et al.* (2009) possesses a crown labiolingually compressed,
347 anteroposteriorly bent, and both carinae serrated. These are features of a ziphodont
348 crown type. Despite its deficient preservation at the level of the cervix, it is possible to
349 estimate its labiolingual compressed (CBR) with a range that varies between 0.48 to 0.5,
350 whereas the ratio CHR is equal to 2.25. In the lateral view, the distal margin is straight,
351 whereas the mesial margin is convex with its apex located centrally in the crown. In

352 mesial and distal views, both carinae are centrally positioned along its margins. Based
353 on the size denticles, they could have extended to the cervix, at least in the mesial
354 carina. In basal view, both lingual and labial surfaces are strongly convex and their
355 faces converge mesially and distally in carinae well visible. Besides, in the cross-section
356 almost at the level of the cervix is lenticular.

357 **Denticles.** The mesial and distal carinae bear 13 denticles per 5 mm at mid-crown.
358 However, the denticle density in the apex of both carinae could not be calculated
359 because these are highly eroded. The same is true for most basal denticles of the mesial
360 carina. The all denticles are symmetrical with its external margin convex.
361 Interdenticular spaces are narrow, measuring less than a third of the width of the
362 denticles.

363 **Crown surface and ornamentation.** In lateral view, the crown has enamel marked
364 wrinkles separated by sulci that traverse continuously the labial and lingual surface.
365 These surfaces are concave towards the base of the tooth on both margins and straight
366 and perpendicular to the major axis of the tooth in the middle of the surface. In the
367 apical area, three denticles are observed between two wrinkles, while in the middle part
368 five denticles are observed between two wrinkles. The relationship between mesial
369 denticles vs. distal (DSDI) obtained in UNPSJB-PV 969 is equal to 1.

370

371 **4.4. Portezuelo Formation**

372 **Theropoda** Marsh, 1881

373 **Ceratosauria** Marsh, 1884

374 **Abelisauroidea** Bonaparte, 1991

375 **Abelisauridae** Bonaparte and Novas, 1995

376 **Gen. and sp. indet.**

377 **Locality and Horizon.** Northern coast of Los Barreales lake area, Futalognko site
378 (38°27'8"S; 68°43'31"W), located at the center of the Neuquén province, Argentina;
379 upper levels of Portezuelo Formation, upper Turonian–lower Coniacian, Upper
380 Cretaceous (Veralli and Calvo, 2004; Garrido, 2010).

381 **State of preservation and general morphology.** All teeth are almost complete and are
382 interpreted as isolated shed tooth crowns. Specimens MUCPv 384, MUCPv 386 and
383 MUCPv 387 are the best preserved teeth, although all lack the basalmost sector of the
384 crown; specimens MUCPv 381 and MUCPv 391 are the most damaged ones. MUCPv
385 381 lacks most of its basal portion, a large portion of the distal margin close to the mid-
386 crown, and its apicalmost sector. MUCPv 391 is represented by a large apical portion of
387 the crown.

388 **Morphotype I**

389 **Material.** MUCPv 381, 384, 386, and 387 (Figure 6).

390 **Crown overall morphology.** Crowns studied here, which integrate the Morphotype I,
391 are considered lateral teeth. They are characterized by an important to normal
392 labiolingual compression at the crown base ($0.48 \leq \text{CBR} \leq 0.55$; Table 1). Basoapically,
393 the mesial margin is strongly convex, whereas the distal margin is straight to slightly
394 concave in lateral view, with the apex almost at the same level of the distal carina. In
395 apical or basal view, both labial and lingual surfaces are mesiodistally convex. The four
396 crowns show well-developed mesial and distal carinae. In the mesial view, the mesial
397 carina is centrally positioned on the mesial margin on some teeth, whereas in MUCPv

398 384 is slightly curved lingually towards the base. In the distal view, the distal carina is
399 straight in almost all crowns, except in MUCPv 384 whose distal carina is strongly
400 bowed labially. The crowns are lenticular to lanceolate in cross-section at the level of
401 the cervix.

402 **Denticles.** On all crowns, the mesial carina bears 11 denticles per 5 mm at mid-crown,
403 whereas the distal carina bears between ten to 12 denticles per 5 mm at mid-crown. The
404 mesial denticles are slightly larger than the distal denticles at the mid-crown and about
405 the same size at the mid-crown (DSDI = 0.9 to 1.09). Both the mesial and distal
406 denticles are chisel-shaped, sub-quadrangular at the base and inclined apically, and their
407 external margin is symmetrically convex. Additionally, the denticles are longer
408 mesiodistally than wide baso-apically. The interdenticular space is narrow and there are
409 not interdenticular sulci between the denticles.

410 **Crown surface and ornamentation.** Marginal undulations, and transverse undulations
411 are present. The texture is irregular and not oriented in any preferential direction.

412

413 **Morphotype II**

414 **Material.** MUCPv 391 (Figure 6).

415 **Crown overall morphology.** Both the mesial and distal margin is strongly apicobasally
416 convex, with the apex positioned almost at the middle of the crown. Both labial and
417 lingual surfaces are mesiodistally convex and the lingual surface is strongly
418 apicobasally concave. The tooth shows well-developed mesial and distal carinae, with
419 well visible denticles and displaced lingually. The crown is salinon-shape (i.e., with
420 labial margin convex and lingual margin biconcave) in cross-section at the mid-crown.

421 **Denticles.** The mesial carina bears 12 denticles per 5 mm at mid-crown, whereas the
422 distal carina bears 11 denticles per 5 mm at mid-crown. The mesial denticles are slightly
423 larger than the distal denticles at the mid-crown to roughly the same size at the mid-
424 crown (DSDI = 0.9). Both the mesial and distal denticles are chisel-shaped, sub-
425 quadrangular at the base and inclined apically, and their external margin is
426 symmetrically convex. The denticles are longer mesiodistally than wide baso-apically.
427 The interdenticular space is narrow and there are not interdenticular sulci between the
428 denticles.

429 **Crown surface and ornamentation.** Marginal undulations are present and well-
430 developed. The texture is irregular and not oriented in any preferential direction.

431

432 **4.5. Plottier Formation**

433 **Theropoda** Marsh, 1881

434 **Ceratosauria** Marsh, 1884

435 **Abelisauroidea** Bonaparte, 1991

436 **Abelisauridae** Bonaparte and Novas, 1995

437 **Gen. and sp. indet.**

438 **Material.** Endemas-Pv 16 (Figure 7).

439 **Locality and Horizon.** El Anfiteatro area, northern of Parrita post locality (39°18'13"S;
440 68°24'35"O), located at the center-west of the Río Negro province, Argentina; Lisandro
441 Formation, upper Coniacian-lowermost Santonian?, Upper Cretaceous (Salgado *et al.*,
442 2009; Garrido, 2010).

443 ***State of preservation and general morphology.*** Endemas-Pv 16 consists of an almost
444 complete tooth that lacks part of the crown base. Although all denticles are worn, some
445 of them present their original form fairly well preserved.

446 ***Crown overall morphology.*** Based on its general morphology, this tooth is considered
447 as a lateral shed tooth. While it is not possible to calculate the exact value of the
448 labiolingual compression of the crown (CBR), said ratio is inferred to be normal (close
449 to 0.52) given that the missing basal sector is negligible. Similar inferences (CHR = 2.4)
450 can be done regarding the baso-apical elongation of the crown based on the parameters
451 provided by Hendrickx and Mateus (2014). The mesial margin of the crown is strongly
452 convex in lateral view with observable serrated carina. The distal margin of the crown is
453 slightly concave in lateral view, also with observable serrated carina. Both in apical and
454 basal view, lingual and labial surfaces are convex and their faces converge mesially and
455 distally in well visible carinae. In cross-section almost at the level of the cervix, the
456 tooth is lenticular to slightly oval. As mentioned by Salgado *et al.* (2009), the mesial
457 carina is straight and located centrally in the mesial margin, whereas distal carina is
458 slightly displaced lingually. Unlike previously reported observations (Salgado *et al.*,
459 2009), the distal carina is not extended to the cervix and it is impossible to determine
460 due to its missing most basal sector. Regarding the mesial carina, this is extended to the
461 cervix.

462 ***Denticles.*** The mesial carina bears 15 denticles per 5 mm at mid-crown, and 18
463 denticles per 5 mm close to the cervix. Since the carina is eroded, the density of
464 denticles close to the apex is unknown. The distal carina possesses 14 denticles per 5
465 mm at mid-crown, 15 denticles per 5 mm close to the apex, and 15 denticles per 5 mm
466 close to the base of the crown. In both carinae, the density of denticles increases apical
467 and basally from mid-crown (DSDI = 0.9). The denticles are chisel-like in shape and

468 slightly inclined towards the apex, and the interdenticular space is narrow, less than
469 one-third of the denticle width.

470 ***Crown surface and ornamentation.*** The enamel texture is smooth, lacking transverse
471 undulations, marginal undulations, flutes, longitudinal grooves, or ridges are absent.

472

473 **4.6. Allen Formation**

474 **Theropoda** Marsh, 1881

475 **Ceratosauria** Marsh, 1884

476 **Abelisauroidea** Bonaparte, 1991

477 **Abelisauridae** Bonaparte and Novas, 1995

478 **Gen. and sp. indet.**

479 ***Material.*** MACN-Pv-RN 1085 (Figure 8).

480 ***Locality and Horizon.*** Bajo de Santa Rosa area, Cerro Bonaparte locality (40°03'25"S;
481 66°47'53"W), located at the center of the Río Negro province, Argentina; lower subunit
482 of the Allen Formation, middle Campanian to lower Maastrichtian, Upper Cretaceous
483 (Martinelli and Forasiepi, 2004; Salgado *et al.*, 2007).

484 ***State of preservation and general morphology.*** MACN-Pv-RN 1086 consists of a
485 fragment of the middle and apical sector of the crown. Both enamel labial and lingual
486 surfaces of the shed tooth are well preserved, as are the denticles.

487 ***Crown overall morphology.*** The crown studied here is interpreted as a mesial tooth
488 based on its general morphology. Given that it lacks the basal sector (i.e., at level of the

489 cervix), it is not possible to measure the crown height, labiolingual compression of the
490 crown, and/or the ratio baso-apical height. Apicobasally, the mesial margin of the crown
491 is slightly convex in lateral view with a present and serrated carina. The distal margin of
492 the crown is straight to slightly convex. Likewise, the carina is present and serrated in
493 the mesial margin. Regarding to apex, is located centrally in the crown. In the apical
494 view, the labial and lingual surfaces are mesiodistally convex, but the lingual surface
495 also is concave apicobasally. In basal view, both lingual and labial surfaces are strongly
496 convex, and their faces converge mesially and distally in well visible carinae. In cross-
497 section at level mid-crown, the tooth is salinon-shaped. In the mesial view, the mesial
498 carina is oriented to the lingual surface. In the distal view, the distal carina is centrally
499 positioned on the crown.

500 ***Denticles.*** The mesial carina bears ten denticles per 5 mm at mid-crown, and nine
501 denticles per 5 mm close to the apex. The distal carina possesses nine denticles per 5
502 mm at mid-crown, and nine denticles per 5 mm close to the apex. The mesial denticles
503 increase toward mid-crown, whereas the distal denticles have the same density (DSDI =
504 0.9). Both mesial and distal denticles are symmetrical to slightly asymmetrically convex
505 with a biconvex external margin. The interdenticular space is narrow, less than one-third
506 of the denticles width. The interdenticular sulci are clearly visible, being long and well-
507 developed.

508 ***Crown surface and ornamentation.*** The crown of the tooth possesses arcuate marginal
509 undulations on the lingual surface about the mesial and distal margin. These are well
510 compacted, abundant and horizontally oriented in mesial sense. Transverse undulations,
511 flutes, longitudinal grooves, or ridges are absent. The enamel texture is smooth to
512 irregular.

513

514 **5. Analysis**

515 **5.1. Cladistic analysis.** The cladistic analysis of the dentition-based yielded 100 most
516 parsimonious trees (MPT) when using the constrained search (namely, CI = 0.198; RI =
517 0.465; L = 1319; strict consensus tree: CI = 0.196; RI = 0.458; L = 1333). The shed
518 tooth CdM (see Table 1) was either recovered within Carcharodontosauridae, as the
519 sister taxon of *Mapusaurus*, or as the sister taxon of a small clade formed by
520 *Giganotosaurus* and *Mapusaurus* in the strict consensus tree (Figure 9). In all of the
521 most parsimonious trees, CLM and PoM2 was either recovered within a small subclade
522 formed by *Skorpiovenator* and *Aucasaurus*, where each operational taxonomic unit is
523 located in different positions between the different more parsimonious trees. Regarding
524 PIM, BBM, PoM1 and AIM was either recovered within a small subclade conformed by
525 *Arcovenator*, *Majungasaurus*, and *Indosuchus*, whose OTUs also variate their positions
526 along the different more parsimonious trees. In this sense, in the strict consensus tree,
527 these specimens were recovered within Abelisauridae and on a polytomy together with
528 *Skorpiovenator*, *Aucasaurus*, *Majungasaurus*, *Indosuchus*, *Chenaniasaurus*, and
529 *Arcovenator* (Figure 9).

530 The cladistic analysis conducted from the dentition-based data matrix without
531 constraints found 100 most parsimonious trees (CI = 0.254; RI = 0.583; L = 1024). The
532 strict consensus tree (CI = 0.178; RI = 0.346; L = 1458) recovered the tooth CdM within
533 clade Carcharodontosauridae, essentially in a polytomy together with *Mapusaurus*,
534 *Carcharodontosaurus*, and *Giganotosaurus* (Figure 10). CLM and PoM2 were
535 recovered in a polytomy with *Skorpiovenator*, whereas PIM, BBM, and PoM1 were
536 recovered closely related to *Indosuchus*. Respect AIM is resolved in a polytomy

537 together with *Aucasaurus*, *Abelisaurus*, *Majungasaurus*, *Rugops*, and *Kryptops* (Figure
538 10).

539 Regarding the cladistic analysis conducted of the tooth-crown-based data matrix
540 without constraints found a poorly resolved strict consensus tree from 100 most
541 parsimonious trees (namely, CI = 0.245; RI = 0.633; L = 652; strict consensus tree: CI =
542 0.112; RI = 0.05; L = 1433). Even though strict consensus tree yielded great polytomy,
543 a better-resolved tree was obtained by pruning *a posteriori* *Limusaurus* (juvenile and
544 adult). In this study, the tooth shed CdM was recovered in a polytomy within
545 Carcharodontosauridae together with *Carcharodontosaurus*, and Giganotosaurini
546 (*Mapusaurus* + *Giganotosaurus*), whereas PIM, BBM, and PoM1 were recovered in a
547 small subclade that contains the abelisaurid *Indosuchus*. CLM and PoM2 were
548 recovered close to the base of Abelisauridae but more derived than *Arcovenator* and
549 *Chenaniasaurus*, whereas AIM was nested in a small polytomy together with
550 *Aucasaurus*, *Majungasaurus*, *Abelisaurus*, *Rugops*, and *Kryptops* (Figure 11).

551 **5.2. Discriminant analysis.** The DFA conducted on the whole dataset classified the
552 shed teeth MDPa-Pv 005 and MACN-Pv-RN 1085 as tyrannosaurids; MUCPv 381,
553 MUCPv 384, MUCPv 386, MUCPv 387 and Endemas-Pv 2 as megalosaurids, and
554 MUCPv 391 and UNPSJB-PV 969 as non-abelisauroid ceratosaurians; and Endemas-Pv
555 16 as a non-tyrannosauroid tyrannosaurid (clade-level analysis; PC1 and PC2 account
556 for 38.19% and 30.88% of the total variance, respectively; Figure 12). MDPa-Pv 005
557 was classified to taxon-level as the carcharodontosaurid *Mapusaurus*; MUCPv 381,
558 MUCPv 391, and MACN-Pv-RN 1085 as abelisaurid *Chenaniasaurus*; MUCPv 384
559 and MUCPv 386 as the ceratosaurid *Genyodectes*; MUCPv 387 as the abelisaurid
560 *Skorpiovenator*; UNPSJB-PV 969 as the ceratosaurian *Berberosaurus*; Endemas-Pv 2 as

561 the allosaurid *Allosaurus*; and Endemas-Pv 16 as indeterminate abelisaurid (PC1 and
562 PC2 account for 35.7% and 27.78% of the total variance, respectively).

563 Reclassification rate (RR) was relatively high (59.25% to clade-level and
564 56.55% to taxon-level). When the discriminant function analyses were conducted if
565 absence of denticles was inapplicable, the RR at the group-level was slightly better
566 (61.88%), whereas at taxon-level was roughly the same (57.46%, see supplementary
567 information). In this analysis, the crowns were classified the same as in previous
568 analysis (clade level; PC1 39.15% and PC2 30.96%). Similarly, all shed crowns were
569 classified the same as in previous analysis at taxon-level (PC1 36.43% and PC2
570 22.58%).

571 In so far as to DFA based on the whole datasets of Hendricks's first-hand
572 measurements (i.e., datasets restricted to taxa with teeth larger than two centimeters),
573 MDPA-Pv 005 was classified as tyrannosaurid; MUCPv 381, MUCPv 384, MUCPv
574 386, MUCPv 387 and MACN-Pv-RN 1085 as megalosaurids; MUCPv 391 and
575 Endemas-Pv 2 as allosaurids, and UNPSJB-PV 969 and Endemas-Pv 16 as
576 metriacanthosaurids (clade level; PC1 47.43% and PC2 27.57%; Figure 13). At, taxon-
577 level, MDPA-Pv 005 was classified as the carcharodontosaurid *Mapusaurus*; MUCPv
578 391 and Endemas-Pv 2 as the allosaurid *Allosaurus*; MUCPv 384 and MUCPv 386 as
579 the megalosaurid *Duriavenator*; MUCPv 381 and MACN-Pv-RN 1085 as the
580 megalosaurid *Torvosaurus*; MUCPv 387, UNPSJB-PV 969 and Endemas-Pv 16 as
581 indeterminate abelisaurids (PC1 and PC2 account for 54.22% and 18.47% of the total
582 variance, respectively). RR are much better at taxon-level than at clade-level (i.e.,
583 61.65% and 58.25%, respectively), however, it are low when compared to the RR when
584 the absence of denticles was considered as inapplicable (61.75% and 60.4%,
585 respectively). In this analysis, the shed tooth MDPA-Pv 005 was classified as a

586 carcharodontosaurid at clade-level, whereas the remaining teeth were classified the
587 same as in the previous analysis (PC1 56.13% and PC2 23.98%). At taxon-level,
588 MUCPv 381 was classified as the megalosaurid *Dubreuillosaurus*, and the crowns
589 remaining were classified the same as in the previous analysis (PC1 45.25% and PC2
590 21.14%).

591 In both analyses, the PC1 summarized a major contribution of the variables
592 CBL, CBW, CH, AL, MCL, MCW, MSL and minor contributions from MDL and
593 DDL. The high positive PC1 scores identified taxa with high and wide teeth, whereas
594 the more negative PPC1 scores set apart taxa with teeth that are short and narrow. The
595 PPC2 summarized a major contribution of the variables LAF and LIF. High positive
596 PC2 scores identified mainly taxa with a major number of flutes on the labial and
597 lingual surfaces of the crown, whereas negative scores characterized taxa with non-
598 number of flutes in both surfaces of the crown.

599

600 **5.3. Cluster analysis.** The cluster analysis using hierarchical clustering option found the
601 tooth MDPA-Pv 005 as the sister taxon of *Acrocanthosaurus*; MUCPv 384 closely
602 related to *Berberosaurus*; MUCPv 386 as *Chenaniasaurus*; MUCPv 387 as
603 *Duriavenator*; UNPSJB-PV 969 as *Ceratosaurus*; Endemas-Pv 2 as *Majungasaurus*;
604 and Endemas-Pv 16 as *Monolophosaurus*. When using the Neighbour-joining clustering
605 option, recoveries MDPA-Pv 005 closely related to *Mapusaurus*, *Giganotosaurus*,
606 *Ceratosaurus* or *Acrocanthosaurus*, MUCPv 384 to *Gorgosaurus*, *Berberosaurus*,
607 *Majungasaurus* or *Carnotaurus*; MUCPv 386 to *Chenanosaurus* or *Duriavenator*;
608 MUCPv 387 to *Carnotaurus* or *Majungasaurus*; UNPSJB-PV 969 to *Ceratosaurus*,
609 Endemas-Pv 2 to *Carnotaurus* or *Majungasaurus*, and Endemas-Pv 16 to *Raptorex* (see

610 supplementary information 2.1). The cluster analysis based on the datasets restricted to
611 taxa with teeth larger than two centimeters. MDPA-Pv 005 was then classified as
612 *Mapusaurus*, *Giganotosaurus*, *Acrocanthosaurus* or *Ceratosaurus*; MUCPv 381 as
613 *Carnotaurus*; MUCPv 384 as *Megalosaurus* or *Duriavenator*; MUCPv 386 as
614 *Duriavenator*; MUCPv 387 as *Megalosaurus* or *Duriavenator*; MUCPv 391 as
615 *Carnotaurus*; UNPSJB-PV 969 as *Ceratosaurus*; Endemas-Pv 2 as *Carnotaurus* or
616 *Majungasaurus*; Endemas-Pv 16 as *Monolophosaurus*; and MACN-Pv-RN 1085 as
617 *Carnotaurus* or *Dubreuillosaurus*. When using the Neighbour-joining clustering option,
618 recoveries of MDPA-Pv 005 were classified as *Acrocanthosaurus*; MUCPv 381 to
619 *Majungasaurus* or *Dubreuillosaurus*; MUCPv 384 as *Berberosaurus* or *Arcovenator*;
620 MUCPv 386 as *Duriavenator*; MUCPv 387 as *Duriavenator*; MUCPv 391 as
621 *Abelisaurus*; UNPSJB-PV 969 as *Ceratosaurus*; Endemas-Pv 2 as *Carnotaurus*;
622 Endemas-Pv 16 as *Marshosaurus*; and MACN-Pv-RN 1085 as *Carnotaurus* or
623 *Dubreuillosaurus* (see supplementary information 2.1).

624

625 **6. Discussion**

626 **6.1. Taxonomic inference of the Candeleros Formation tooth MDPA-Pv 005**

627 From the obtained results, the three cladistic analyses allow to assign with
628 confidence MDPA-Pv 005 as a tooth likely belonging to carcharodontosaurid. In all
629 analyses it is recovered as a derived carcharodontosaurid within Carcharodontosauridae
630 clade (*sensu* Novas *et al.*, 2013). In fact, the DFAs and cluster analysis recovered the
631 same results supporting the affinity of the shed tooth as carcharodontosaurid (see
632 supplementary information). Regarding the plot generated from the DFA performed on
633 the two datasets, it is observed that MDPA-Pv 005 is placed outside the occupied

634 morphospace by the different groups now, but close to the morphospace of
635 Tyrannosauridae and Carcharodontosauridae, or, depending on the analysis, just near
636 the edge of Tyrannosauridae; depending on the analysis (Figures 12 and 13).

637 Both Tyrannosauridae and Carcharodontosauridae possess lateral dentition with
638 a CH, CBR, and CHR with slightly similar variation ranges, i.e., crowns with height
639 higher to 6 cm, labiolingual compression of the crown that variates between ~0.4 to
640 ~0.65 (in carcharodontosaurids) and ~0.4 to ~0.8 (in tyrannosaurids), and baso-apical
641 elongation of the crown which varies between ~1.14 to ~2.3 (in carcharodontosaurids)
642 and ~1.3 to ~2.75 (in tyrannosaurids). Nevertheless, the size differences between mesial
643 and distal denticles differ lateral teeth of carcharodontosaurids and tyrannosaurids.
644 Indeed, mesial and distal denticles are nearly the same size in tyrannosaurids, whereas
645 the mesial denticles are larger than the distal in carcharodontosaurids as occurs in the
646 Patagonian forms (i.e., *Mapusaurus* and *Giganotosaurus*, but unknown for
647 *Lajasvenator*; see Coria *et al.*, 2020). In tyrannosaurids, the mesial carina strongly twist
648 onto the mesiolingual surface, whereas that in carcharodontosaurids the mesial carina is
649 centrally positioned on mesial margin or is weakly curved lingually towards the base
650 (Hendrickx *et al.*, 2019). The distal carina in carcharodontosaurids is centrally
651 positioned or slightly displaced, whereas in tyrannosaurids is strongly labially deflected
652 (Hendrickx *et al.*, 2019). Moreover, in lateral teeth of the carcharodontosaurids have a
653 clearly observable braided enamel texture is clearly observed, whereas the
654 tyrannosaurids possess irregular enamel texture (Hendrickx *et al.*, 2019).

655 **6.2. Taxonomic inference of remaining teeth**

656 The results of the three cladistic analyses support the affinity of the Cerro
657 Lisandro, Bajo Barreal, Portezuelo (Morphotype I and II), Plottier, and Allen

658 Morphotypes with the typical dentition of Abelisauridae. Nevertheless, the DFAs and
659 cluster analyses recovered poorly robust results, i.e., the crowns being assigned to
660 Megalosauridae, Allosauridae, Abelisauridae, Carcharodontosauridae, and
661 Tyrannosauridae. The most plausible explanation is that these mixed results are due to
662 the small number of variables measured (see Table 1). On the other hand, the plot
663 generated from the DFA on the two datasets is placed within the morphospace (convex
664 hull) occupied by a high number of theropod groups, including Abelisauridae,
665 Megalosauridae, Tyrannosauridae, Metricanthosauridae, non-abelisauroid Ceratosauria,
666 and Allosauridae (Figures 12 and 13).

667 Unlike Veralli and Calvo (2004), we recognize the specimens MUCPv 381,
668 MUCPv 384, MUCPv 386, and MUCPv 387 as lateral teeth, while MUCPv 391 is
669 recognized as a mesial tooth. These authors argue that all these dental pieces possess
670 enamel wrinkles while we observe that MUCPv 387 lacks both marginal undulations as
671 well as transversal undulations. Furthermore, the only specimens that have marginal
672 undulations in their crowns are MUCPv 381 and MUCPv 391. In the first specimen,
673 these are arranged on both sides adjacent to the distal carina. In the second, they are
674 only present on the lingual face and adjacent to both carinae, although those that are
675 arranged in the mesial carina are more subtle than in the distal carina. Regarding
676 MUCPv 384 and MUCPv 386 specimens are characterized to possess transversal
677 undulations about in the labial face. Unlike Martinelli and Forasiepi (2004), Casal *et al.*
678 (2009) and Salgado *et al.* (2009), we recognize the specimens UNPSJB-PV 969 and
679 Endemas-Pv 16 as lateral teeth, whereas the specimens Endemas-Pv 2 and MACN-Pv-
680 RN 1085 as mesial teeth based on their typical morphology (see Hendrickx *et al.*, 2015).

681 The specimens studied here, and previously reported, are partially complete and
682 well-preserved theropod teeth. However, previously reports on these teeth focused their

683 description and comparison on carcharodontosaurid taxa known at that time. Based on
684 the presence of the arcuate marginal undulations visible on the crowns, the previous
685 authors mention that this unique feature unites these teeth to Carcharodontosauridae and
686 at the same time separates them from other clades of theropods.

687 In summarizing, the shed teeth of Cerro Lisandro, Bajo Barreal, Portezuelo,
688 Plottier and Allen formations have an unique combination of features only observed in
689 the dentition of abelisaurids. The lateral teeth are characterized by a weakly convex
690 distal profile to almost straight, arcuate marginal undulations and transversal
691 undulations; a mesial carina extending to the cervix or just above it; a centrally placed
692 distal carina on the distal margin; symmetrically convex labial and lingual surfaces of
693 the crown in the mesiodistal plane; apically inclined distal denticles and short
694 interdenticular sulci between both mesial and distal denticles; and irregular, non-
695 oriented texture of enamel (see Hendrickx *et al.*, 2019, 2020). Specimens considered
696 here as mesial teeth also possess a combination of features observed in abelisaurids. For
697 example, they present a salinon-shaped cross-section outline, and apically hooked-
698 shaped denticles (see Hendrickx *et al.*, 2019, 2020).

699 An interesting fact that has been registered to date is the tendency to
700 homogenization materials that come from the same stratigraphic unit. In this sense, the
701 teeth from Allen Formation collected in Lago Pellegrini in northern, Río Negro
702 Province, and deposited in the MPCA collections have been referred by Hendrix and
703 Mateus (2014) to *Abelisaurus comahuensis*, because they come from the same area and
704 stratigraphic unit. This assignment has been followed by subsequent works based on
705 this dataset (i.e., Hendrix *et al.*, 2015ab, Gerke and Wings, 2016; Hendrix *et al.*, 2020).
706 Here, we consider it as a composite OTU in accordance with previous authors, but the

707 referral of the Lago Pellegrini teeth to *Abelisaurus comahuensis* has to be revised in
708 more detail.

709

710 **6.3. Biostratigraphic implicances**

711 The fossil record of middle to large bodied predators during the late Mesozoic has
712 increased notably during the last decades, especially in Gondwanan landmasses,
713 allowing to infer about the composition and evolution of their terrestrial faunas (i.e.
714 Krause *et al.*, 2007; Novas, 2013; Ibrahim *et al.*, 2020). Patagonia, as the southern
715 region of South America, has been considered to represent the consecutive changes of
716 faunistic realms, following the successive paleobiogeographic scenarios relative to the
717 fragmentation of Gondwana, intercontinental dispersal events, and still disputable
718 regional isolation into the continent (i.e., Sereno *et al.*, 2004; Coria and Salgado, 2005).
719 The upper Mesozoic Patagonian theropod record includes elements from the Upper
720 Jurassic of the Cañadón Calcareo and Toqui formations, consisting of basal tetanurans
721 of uncertain or debated relationships (Novas *et al.*, 2015; Rauhut and Pol, 2017). The
722 lowermost Cretaceous (Berriasian to Barremian) theropod record is contained in the
723 Bajada Colorada, Mulichinco and La Amarga formations, and consists of noosaurid and
724 abelisaurid ceratosaurs, megalosauroids and a basal carcharodontosaurid, *Lajasvenator*
725 *ascheriae* (Bonaparte, 1996; Apesteguía and Bonaparte, 2004; Canale *et al.*, 2017;
726 Coria *et al.*, 2020). *Lajasvenator* represents the ancient proper Carcharodontosauridae
727 (sensu Benson *et al.*, 2010). It appears to be included in a monophyletic group together
728 with the african *Eocarcharia dinops* and the european *Concavenator corcovatus*, which
729 in turns represent an early branch of the lineage of more derived taxa.

730 During the late Early Cretaceous and at the beginning of the Late Cretaceous
731 (Aptian to middle Turonian), Patagonia contained a particular fauna with strong
732 similarities with those of northern Africa (i.e., Leanza *et al.*, 2004; Coria and Salgado,
733 2005; Krause *et al.*, 2020). This fauna, called by Krause and colleagues the “Middle
734 Cretaceous Faunal Assemblage of Gondwana” (MCFAG) (Krause *et al.*, 2020), is
735 represented by multiple lithostratigraphic units, including Cerro Barcino, Matasiete,
736 Mata Amarilla, Lohan Cura, Rayoso, Candeleros, Huincul and Bajo Barreal formations.
737 Their theropod faunas includes ceratosaurids, elaphrosaurine noosaurids and non-
738 furileusaurian abelisaurids among ceratosaurians (Martínez *et al.*, 1986; Coria and
739 Salgado, 1998; Rauhut, 2004; Canale *et al.*, 2009; Juárez Valieri *et al.*, 2011; Baiano *et*
740 *al.*, 2020; Cerroni *et al.*, 2020), the enigmatic bahariasaurids (Apesteguía *et al.*, 2016;
741 Motta *et al.*, 2020), and multiple tetanuran lineages, as carcharodontosaurids (Coria and
742 Salgado, 1995; Novas *et al.*, 2005; Coria and Currie, 2006; Motta *et al.*, 2016), basal
743 coelurosaurs (Martínez and Novas, 2006; Novas *et al.*, 2012), megaraptorans (Casal *et*
744 *al.*, 2016; Motta *et al.*, 2016), basal alvarezsaurians (Makovicky *et al.*, 2012), and non-
745 avian paravians including basal unenlagiids (Makovicky *et al.*, 2005; Motta *et al.*,
746 2020).

747 Within this assemblage, the carcharodontosaurids are represented by the highly
748 derived Giganotosaurini clade, with the early record of the Albian *Tyrannotitan*
749 *chubutensis*, *Giganotosaurus carolini* from early to middle Cenomanian and the slightly
750 younger *Mapusaurus roseae* and their possible junior synonym *Taurovenator violantei*
751 (Coria *et al.*, 2020) from the late Cenomanian to early Turonian. *Mapusaurus roseae* and
752 *T. violantei* constitute the last convincing evidence of this lineage of large predators in
753 Patagonia and South America. At this stage, theropods are represented by for particular
754 sauropod lineages, including a high diversity of rebbachisaurid diplodocoids, basal

755 titanosaurs and giant non-lognkosaurid colossosaurians (Martínez *et al.*, 2016; Canudo
756 *et al.*, 2018; Simón *et al.*, 2018). The crocodyliformes are represented primarily by
757 uruguaysuchids (Fernández Dumont *et al.*, 2020).

758 A critical issue about the changes in the faunistic conformation of the
759 Cretaceous faunas from Patagonia and even South America is the faunistic turnover
760 from the “middle” to Late Cretaceous faunas from the Neuquén Basin that has been
761 previously suggested (i.e., Coria and Salgado, 2005) which involve extinctions of some
762 lineages and subsequent adaptive radiation of others. The persistence of lineages such as
763 ceratosaurids, elaphrosaurine noosaurids and carcharodontosaurids, but also
764 rebbachisaurid and basal titanosaurian among sauropods and uruguaysuchid
765 mesoeucrocodylians, represents common components of the MCFAG that disappear
766 from the fossil record of Patagonia, as well as from northern South America, Africa and
767 Europe posterior to this stage. Several clades appear to generate a radiation of taxa just
768 posterior to the end of the MCFAG in South America and particularly in Patagonia. An
769 early stage of the fauna from South America posterior to the isolation of the continent
770 with Africa, defined as the “Late Cretaceous Faunal Assemblage of South America”
771 (LCFASA), is characterized by the presence of furileusaurian abelisaurids (Filippi *et al.*,
772 2016), as well as megaraptorids in the theropod component (Porfiri *et al.*, 2018), the
773 radiation of patagonykine alvarezsaurians and derived unenlagiids (Novas *et al.*, 2013)
774 among the theropod dinosaurs, multiple lineages of small sized derived titanosaurs and
775 long-spined lognkosaurids among sauropods (Carballido *et al.*, 2017) large sized
776 elasmarians (Cruzado Caballero, 2019; Ibiricu *et al.*, 2020) and peirosaurids, advanced
777 notosuchians and baurusuchids among the mesoeucrocodylians (Pol and Leardi, 2015).

778 In this context, the subsistence of the carcharodontosaurid lineage in Patagonia
779 was proposed multiple times based on the assignation of the isolated teeth discussed in

780 the present study, which approach them methodologically for first time, by multivariate
781 analysis. In fact, the recovery of the all previously purported carcharodontosaurid
782 evidence posterior to the MCFAG from Patagonia results in the current study as
783 belonging to abelisaurid theropods, in accordance with the hypothesis of the local
784 extinction of the carcharodontosaurid theropods of Patagonia as part of a faunistic
785 turnover apparently occurred between the late Turonian to early Coniacian.

786 Since the Neuquén Basin contains a succession of terrestrial vertebrate faunas
787 during most of the Late Cretaceous, it is the best resource for biostratigraphic
788 inferences. All the lineages representing the MCFAG previously discussed, including
789 the carcharodontosaurids, are limited to the Huincul Formation. The overlying Cerro
790 Lisandro Formation tetrapod fossil record, although less diverse than their underlying
791 Huincul Formation and the overlying Portezuelo Formation, appears to have a
792 fossiliferous record that is more closely related to the last one because of presence of
793 peirosaurids, elasmarians and high-spined lognkosaurians. Therefore, the assignment of
794 the Cerro Lisandro morphotype tooth to Abelisauridae instead of
795 Carcharodontosauridae is concordant with this scenario. We consider the more diverse
796 fauna recorded in the Portezuelo Formation, and its highly abundant fossiliferous
797 record, as depicting a clearly differentiated fauna from those of the MCFAG, and
798 representing the first clear stages of the denominated “Late Cretaceous Faunal
799 Assemblage of South America” (LCFASA).

800 The assignation of the Portezuelo Formation morphotype teeth, as also those of
801 the Plottier and Allen formations, to Abelisauridae leave without support the idea of
802 survival of the carcharodontosaurids in Patagonia posterior to the MCFAG to LCFASA
803 faunistic turnover. We consider that previous assumptions of the time of the events
804 posterior to the deposition of the Portezuelo Formation in the Neuquén Basin (Coria and

805 Salgado, 2005) are incorrect. Instead, we propose that the faunistic turnover occurred
806 previous to the deposition of the Portezuelo Formation, more precisely at the end of the
807 deposition of the Huincul Formation and at the beginning or during the deposition of the
808 Cerro Lisandro Formation, approximately in the late Turonian–earliest Coniacian.

809 On the other hand, the southern Golfo San Jorge Basin present in the Bajo
810 Barreal a composition with mixed components, including rebbachisaurid and basal
811 titanosaurs, that has typical components of the MCFAG and other more reminiscent
812 to those of the LCFASA, with large clawed megaraptorans and elasmarians. In this
813 context, the assignation of the Bajo Barreal morphotype tooth to abelisaurid is not
814 unexpected, but it could be interpreted both as evidence of a slightly younger age of the
815 Bajo Barreal Formation respect to the Huincul Formation or simply is part of the
816 composition of a proper MCFAG, which already includes the abelisaurids. This is in
817 accordance with previous faunistic comparisons between the Neuquén and Golfo San
818 Jorge Basins (Canale *et al.*, 2011; Ibiricu *et al.*, 2020).

819 The geographical range can in fact not be restricted to Patagonia but cover even
820 completely to South America, as indicated by the faunistic composition of the Salta, La
821 Rioja and equivalent basins from northwestern Argentina (Novas and Agnolín, 2004;
822 Agnolín and Chiarelli, 2010; D’Emic and Wilson, 2011; Fiorelli *et al.*, 2016;
823 Hechenleitner *et al.*, 2018, 2020), the Norte Basin of western Uruguay (Perea *et al.*,
824 2011) or Bauru Basin faunas of Brazil (Martinelli and Teixeira, 2015; Brusatte *et al.*,
825 2017; Grillo and Delcourt, 2017; Geroto and Bertini, 2019; Langer *et al.*, 2019).
826 However, the composition of some of these faunas during the Turonian-Santonian lapse
827 is poorly or completely unknown. In the case of the Bauru Basin faunal assemblages,
828 similar detailed analyses of dental and cranial material previously proposed as

829 belonging to carcharodontosaurids has been conclusive in discarding this assignment
830 (Delcourt and Grillo, 2018; Delcourt *et al.*, 2020).

831

832 **7. Conclusions**

833 Our results, based on data obtained from cladistic analyses, DFAs, and cluster
834 analyses, suggest that isolated shed tooth MDPa-Pv 005 of Candeleros Formation
835 (lower Cenomanian) can be assigned to a carcharodontosaurid lateral tooth. However,
836 remaining specimens previously considered as carcharodontosaurids actually belong to
837 abelisaurids. In the case of Portezuelo teeth (upper Turonian to lower Coniacian) where
838 two morphotypes have been found, they could even correspond to different positions
839 within the tooth row of a single taxon. Even though the cladistic analysis was more
840 precise and exact in comparison with the DFAs and cluster analyses, the latter should
841 not be discarded. The lack of conclusive evidence could have been caused by a number
842 of variables that could not be measured.

843 While this study supports not only the previous idea that, although
844 morphologically distinct, carcharodontosaurids and abelisaurids share similar traits, it
845 also supports the notion that carcharodontosaurids became extinct in South America
846 during the late Turonian and were replaced by other large theropods such as
847 megaraptorids and abelisaurids. The extinction of carcharodontosaurids in Patagonia, as
848 well as in northern South America, are indicative of the faunal turnover event from the
849 “Middle Cretaceous Faunal Assemblage of Gondwana” (MCFAG) to the early stages of
850 the “Late Cretaceous Faunal Assemblage of South America” (LCFASA).

851

852

853 **Acknowledgments**

854 We thank Ludmila Coria and Jorge Calvo for allowing access to materials under
855 their care. To Lucas Fiorelli, Fernando Novas, Leonardo Salgado, and Matías Soto for
856 further information of materials and biostratigraphic aspects discussed in this
857 manuscript. We are particularly grateful to E. Koutsoukos and R. Delcourt for their
858 insightful reviews which greatly improved the manuscript. Also, we thank C. Giai that
859 assisted with English editing.

860

861 **References**

- 862 Agnolín, F.L., Chiarelli, P., 2010. The position of the claws in Noosauridae (Dinosauria:
863 Abelisauroidea) and its implications for abelisauroid manus evolution.
864 *Paläontologische Zeitschrift* 84, 293–300.
- 865 Andreis, R.R. 2001. Paleocology and environments of the Cretaceous Sedimentary
866 Basin of Patagonia (Southern Argentina). Buenos Aires, VII International
867 Symposium on Mesozoic Terrestrial Ecosystems. *Asociación Paleontológica*
868 *Argentina*. 7(1), 7-14.
- 869 Apesteguía, S. 2007. The sauropod diversity of the La Amarga Formation (Barremian),
870 Neuquén (Argentina). *Gondwana Research*, 12(4), 533-546.
- 871 Apesteguía, S., Smith, N.D., Juárez Valieri, R.D., Makovicky, P.J., 2016. An unusual
872 new theropod with a didactyl manus from the Upper Cretaceous of Patagonia,
873 Argentina. *PLoS ONE* 11, e0157793.

- 874 Benson, R.B.J., Carrano, M.T., Brusatte, S.L., 2010. A new clade of archaic large-
875 bodied predatory dinosaurs (Theropoda: Allosauroida) that survived to the
876 latest Mesozoic. *Naturwissenschaften* 97, 71–78.
- 877 Bonaparte, J.F. 1997. *Rayososaurus agrioensis* Bonaparte, 1995. *Ameghiniana* 34: 116
- 878 Brusatte, S. L., and Carr, T. D. 2016. The phylogeny and evolutionary history of
879 tyrannosauroid dinosaurs. *Sci. Reports*, 6, 20252.
- 880 Brusatte, S. L., and Sereno, P. C. 2008. Phylogeny of Allosauroida (Dinosauria:
881 Theropoda): comparative analysis and resolution. *J. Syst. Palaeontol.* 6(2), 155-
882 182.
- 883 Brusatte, S. L., Benson, R. B. J., Carr, T. D., Williamson, T. E., and Sereno, P. C. 2007.
884 The systematic utility of theropod enamel wrinkles. *Journal of Vertebrate*
885 *Paleontology*, 27(4), 1052-1056.
- 886 Brusatte, S. L., Benson, R. B. J., Chure, D.J., Xu, X., Sullivan, C., and Hone, D. W. E.
887 2009. The first definitive carcharodontosaurid (Dinosauria: Theropoda) from
888 Asia and the delayed ascent of tyrannosaurids. *Naturwissenschaften.* 96:1051–
889 1058.
- 890 Brusatte, S.L., Candeiro, C.R. dos A., Simbras, F.M., 2017. The last dinosaurs of Brazil:
891 The Bauru Group and its implications for the end-Cretaceous mass extinction.
892 *An. da Acad. Bras. Ciencias* 89, 1465–1485.
- 893 Calvo, J. O., and Bonaparte, J. F. 1991. *Andesaurus delgadoi* gen. et. sp. nov.
894 (Saurischia-Sauropoda), dinosaurio Titanosauridae de la Formación Río Limay
895 (Albiano-Cenomaniano), Neuquén, Argentina. *Ameghiniana*, 28, 303-310.

- 896 Calvo, J. O., Rubilar-Rogers, D., and Moreno, K. (2004). A new abelisauridae
897 (Dinosauria: Theropoda) from northwest Patagonia. *Ameghiniana*, 41(4), 555-
898 563.
- 899 Canale, J. I., Scanferla, C. A., Agnolin, F. L., and Novas, F. E. 2009. New
900 carnivorous dinosaur from the Late Cretaceous of NW Patagonia and the
901 evolution of abelisaurid theropods. *Naturwissenschaften*, 96(3), 409.
- 902 Canale, J.I., Ibiricu, L.M., Haluza, A., Casal, G.A., 2011. The continental Cenomanian
903 of Patagonia: a comparison between the fossil vertebrate faunas of the Río
904 Limay subgroup (Neuquén Group) and the Bajo Barreal Formation (Chubut
905 Group) fossil vertebrate faunas, in: 4° Congreso Latinoamericano de
906 Paleontología de Vertebrados. San Juan, Argentina, p. 2006.
- 907 Canale, J. I., Carballido, J. L., Otero, A., Canudo, J. I., and Garrido, A. 2014.
908 Carcharodontosaurid teeth associated with titanosaur carcasses from the Early
909 Cretaceous (Albian) of the Chubut Group, Chubut Province, Patagonia,
910 Argentina (p. 23). Neuquén: 28° Jornadas Argentinas de Paleontología de
911 Vertebrados.
- 912 Canudo Sanagustín, J.I., Carballido, J.L., Garrido, A.C., Salgado, L., 2018. A new
913 rebbachisaurid sauropod from the Aptian-Albian, Lower Cretaceous Rayoso
914 Formation, Neuquén, Argentina. *Acta Palaeontol. Pol.* 63, 679–691.
- 915 Carballido, J.L., Pol, D., Otero, A., Cerda, I.A., Salgado, L., Garrido, A.C., Ramezzani,
916 J., Cúneo, R.N., Krause, J.M., 2017. A new giant titanosaur sheds light on body
917 size evolution amongst sauropod dinosaurs. *Proc. R. Soc. London B Biol. Sci.*
918 284, 20171219.

- 919 Carrano, M. T., Benson, R. B., and Sampson, S. D. 2012. The phylogeny of Tetanurae
920 (Dinosauria: Theropoda). *Journal of Systematic Palaeontology*, 10(2), 211-300.
- 921 Casal, G., Candeiro, C. R. A., Martínez, R., Ivany, E., and Ibiricu, L. 2009. Dientes de
922 Theropoda (Dinosauria: Saurischia) de la Formación Bajo Barreal, Cretácico
923 Superior, Provincia del Chubut, Argentina. *Geobios*, 42(5), 553-560.
- 924 Casal, G.A., Martínez, R.D., Luna, M., Ibiricu, L.M., 2016. Ordenamiento y
925 caracterización faunística del Cretácico Superior del Grupo Chubut, Cuenca del
926 Golfo San Jorge, Argentina. *Rev. Bras. Paleontol.* 19, 53–70.
- 927 Cau, A., Beyrand, V., Voeten, D. F. A. E., Fernandez, V., Tafforeau, P., Stein, K.,
928 Barsbold, R., Tsogtbaatar, Kh., Currie, P. J., and Godefroit, P. 2017.
929 Synchrotron scanning reveals amphibious ecomorphology in a new clade of
930 bird-like dinosaurs. *Nature* 552(7685):395-399.
- 931 Cerroni, M.A., Motta, M.J., Agnolín, F.L., Aranciaga Rolando, A.M., Brissón Egli, F.,
932 Novas, F.E., 2020. A new abelisaurid from the Huincul Formation
933 (Cenomanian-Turonian; Upper Cretaceous) of Río Negro province, Argentina. *J.*
934 *South Am. Earth Sci.* 98, 102445.
- 935 Coria, R. A., and Salgado, L. 1995. A new giant carnivorous dinosaur from the
936 Cretaceous of Patagonia. *Nature*, 377(6546), 224-226.
- 937 Coria, R.A., Salgado, L., 1998. A basal Abelisauria Novas, 1992 (Theropoda-
938 Ceratosauria) from the Cretaceous of Patagonia, Argentina, in: Pérez-Moreno,
939 B.P., Holtz, T.R.J., Sanz, J.L., Moratalla-García, J.J. (Eds.), Aspects of the
940 Theropod Paleobiology - Gaia. pp. 89–102.

- 941 Coria, R.A., Salgado, L., 2005. Mid-Cretaceous turnover of saurischian dinosaur
942 communities: evidence from the Neuquén Basin, in: Veiga, G.D., Spalletti, L.A.,
943 Howell, J.A., Schwarz, E. (Eds.), 2. The Neuquén Basin, Argentina: A Case
944 Study in Sequence Stratigraphy and Basin Dynamics - 1. Geological Society of
945 London Special Publication. pp. 317–327.
- 946 Coria, R. A., and Currie, P. J. 2006. A new carcharodontosaurid (Dinosauria,
947 Theropoda) from the Upper Cretaceous of Argentina. *Geodiversitas*, 28(1), 71-
948 118.
- 949 Coria, R. A., Currie, P. J., Ortega, F., and Baiano, M. A. 2019. An Early Cretaceous,
950 medium-sized carcharodontosaurid theropod (Dinosauria, Saurischia) from the
951 Mulichinco Formation (upper Valanginian), Neuquén Province, Patagonia,
952 Argentina. *Cretaceous Research*, 104319.
- 953 Cruzado-Caballero, P., Gasca Pérez, J.M., Filippi, L.S., Cerda, I.A., Garrido, A.C.,
954 2019. A new ornithopod dinosaur from the Santonian of Northern Patagonia
955 (Rincón de los Sauces, Argentina). *Cretac. Res.* 98, 211–229.
- 956 Csiki-Sava, Z., Brusatte, S. L. and Vasile, Ş. 2016. “*Megalosaurus cf. superbus*” from
957 southeastern Romania: The oldest known Cretaceous carcharodontosaurid
958 (Dinosauria: Theropoda) and its implications for earliest Cretaceous Europe-
959 Gondwana connections. *Cretaceous Research* 60: 221–238.
- 960 Cuesta, E., Ortega, F., and Sanz, J. L. 2018a. Appendicular osteology of *Concavenator*
961 *corcovatus* (Theropoda: Carcharodontosauridae) from the Lower Cretaceous of
962 Spain. *Journal of Vertebrate Paleontology*, 38(4), 1-24.

- 963 Cuesta, E., Vidal, D., Ortega, F., and Sanz, J. L. 2018b. The cranial osteology of
964 *Concavenator corcovatus* (Theropoda; Carcharodontosauria) from the Lower
965 Cretaceous of Spain. *Cretaceous Research*, 91, 176-194.
- 966 Currie, P. J., and Zhao, X. J. 1993. A new carnosaur (Dinosauria, Theropoda) from the
967 Jurassic of Xinjiang, People's Republic of China. *Canadian Journal of Earth
968 Sciences*, 30(10), 2037-2081.
- 969 D'Emic, M.D., Wilson, J.A., 2011. New remains attributable to the holotype of the
970 sauropod dinosaur *Neuquensaurus australis*, with implications for saltosaurine
971 systematics - *Acta Palaeontologica Polonica*. *Acta Palaeontol. Pol.* 56, 61–73.
- 972 Delcourt, R., Grillo, O.N., 2018. Reassessment of a fragmentary maxilla attributed to
973 Carcharodontosauridae from Presidente Prudente Formation, Brazil. *Cretac.
974 Res.* 84, 515–524.
- 975 Delcourt, R., Brilhante, N.S., Grillo, O.N., Ghilardi, A.M., Augusta, B.G., Ricardi-
976 Branco, F., 2020. Carcharodontosauridae theropod tooth crowns from the Upper
977 cretaceous (Bauru Basin) of Brazil: A reassessment of isolated elements and its
978 implications to palaeobiogeography of the group. *Palaeogeogr. Palaeoclimatol.
979 Palaeoecol.* 556, 109870.
- 980 Ezcurra, M. D. 2017. A new early coelophysoid neotheropod from the Late Triassic of
981 northwestern Argentina. *Ameghiniana*, 54(5), 506-538.
- 982 Fernández Dumont, M.L., Bona, P., Pol, D., Apesteguía, S., 2020. New anatomical
983 information on *Araripesuchus buitreaensis* with implications for the
984 systematics of Uruguaysuchidae (Crocodyliforms, Notosuchia). *Cretac. Res.*
985 113, 104494.

- 986 Filippi, L.S., Méndez, A.H., Juárez Valieri, R.D., Garrido, A.C., 2016. A new
987 brachyrostran with hypertrophied axial structures reveals an unexpected
988 radiation of latest Cretaceous abelisaurids. *Cretac. Res.* 61, 209–219.
- 989 Fiorelli, L.E., Leardi, J.M., Hechenleitner, E.M., Pol, D., Basilici, G., Grellet-Tinner,
990 G., 2016. A new Late Cretaceous crocodyliform from the western margin of
991 Gondwana (La Rioja Province, Argentina). *Cretac. Res.* 60, 194–209.
- 992 Garrido, A.C., 2010. Estratigrafía del Grupo Neuquén, Cretácico Superior de la Cuenca
993 Neuquina (Argentina): nueva propuesta de ordenamiento litoestratigráfico.
994 *Revista del Museo Argentino Ciencias Naturales*, 12(2), 121–177.
- 995 Gauthier, J. 1986. Saurischian monophyly and the origin of birds. *Memoirs of the*
996 *Californian Academy of Science* 8:1–55.
- 997 Gerke, O., and Wings, O. 2016. Multivariate and cladistic analyses of isolated teeth
998 reveal sympatry of theropod dinosaurs in the Late Jurassic of Northern
999 Germany. *PloS one*, 11(7), e0158334.
- 1000 Geroto, C.F.C., Bertini, R.J., 2019. New material of *Pepesuchus* (Crocodyliformes;
1001 Mesoeucrocodylia) from the Bauru Group: implications about its phylogeny and
1002 the age of the Adamantina Formation. *Zool. J. Linn. Soc.* 185, 312–334.
- 1003 Goloboff, P. A., Farris, J. S. and Nixon, K. C. 2008. TNT, a free program for
1004 phylogenetic analysis. *Cladistics* 24: 774-786.
- 1005 Grillo, O.N., Delcourt, R., 2017. Allometry and body length of abelisauroid theropods:
1006 *Pycnonemosaurus nevesi* is the new king. *Cretac. Res.* 69, 71–89.

- 1007 Hammer, Ø., Harper, D. A., and Ryan, P. D. 2001. PAST: Paleontological statistics
1008 software package for education and data analysis. *Palaeontologia electronica*,
1009 4(1), 9.
- 1010 Hechenleitner, E.M., Fiorelli, L.E., Martinelli, A.G., Grellet-Tinner, G., 2018.
1011 Titanosaur dinosaurs from the Upper Cretaceous of La Rioja province, NW
1012 Argentina. *Cretac. Res.* 85, 42–59.
- 1013 Hechenleitner, E.M., Leuzinger, L., Martinelli, A.G., Rocher, S., Fiorelli, L.E., Taborda,
1014 J.R.A., Salgado, L. 2020. Two Late Cretaceous sauropods reveal titanosaurian
1015 dispersal across South America. *Communications Biology* 3, 622.
- 1016 Hendrickx, C., Mateus, O., and Araújo, R. 2014. The dentition of megalosaurid
1017 theropods. *Acta Palaeontologica Polonica*, 60(3), 627-642.
- 1018 Hendrickx, C., Mateus, O. and Araújo, R. 2015a. A proposed terminology of theropod
1019 teeth (Dinosauria, Saurischia). *Journal of Vertebrate Paleontology* 35: e982797.
- 1020 Hendrickx, C., Mateus, O., Araújo, R., 2015b. The dentition of Megalosauridae
1021 (Theropoda: Dinosauria). *Acta Palaeontologica Polonica* 60 (3), 627-642.
1022 <https://doi.org/10.4202/app.00056.2013>
- 1023 Hendrickx, C., Mateus, O., Araújo, R., and Choiniere, J. 2019. The distribution of
1024 dental features in non-avian theropod dinosaurs: Taxonomic potential, degree of
1025 homoplasy, and major evolutionary trends. *Palaeontologia Electronica*, 22(3).
- 1026 Hendrickx, C., Tschopp, E., and Ezcurra, M. 2020. Taxonomic identification of isolated
1027 theropod teeth: the case of the shed tooth crown associated with *Aerosteon*

- 1028 (Theropoda: Megaraptora) and the dentition of Abelisauridae. *Cretaceous*
1029 *Research*, 104312.
- 1030 Ibiricu, L.M., Casal, G.A., Martínez, R.D., Alvarez, B.N., Poropat, S.F., 2020. New
1031 materials and an overview of Cretaceous vertebrates from the Chubut Group of
1032 the Golfo San Jorge Basin, central Patagonia, Argentina. *J. South Am. Earth Sci.*
1033 98, 102460.
- 1034 Ibrahim, N., Sereno, P.C., Varricchio, D.J., Martill, D.M., Dutheil, D.B., Unwin, D.M.,
1035 Baidder, L., Larsson, H.C.E., Zouhri, S., Kaoukaya, A., 2020. Geology and
1036 paleontology of the Upper Cretaceous Kem Kem Group of eastern Morocco. 1.
1037 *ZooKeys* 928, 1–216.
- 1038 Juárez Valieri, R.D., Porfiri, J.D., Calvo, J.O., 2011. New Information on
1039 *Ekrixinatosaurus novasi* Calvo et al 2004, a giant and massively-constructed
1040 Abelisauroid from the “Middle Cretaceous” of Patagonia, in: Calvo, J.O.,
1041 Porfiri, J.D., González Riga, B.J., Dos Santos, D.D. (Eds.), *Paleontología y*
1042 *Dinosaurios desde América Latina*. pp. 161–169.
- 1043 Krause, D.W., Sampson, S.D., Carrano, M.T., O’Connor, P.M., 2007. Overview of the
1044 history of discovery, taxonomy, phylogeny, and biogeography of *Majungasaurus*
1045 *crenatissimus* (Theropoda: Abelisauridae) from the Late Cretaceous of
1046 Madagascar. 2. *Majungasaurus crenatissimus* (Theropoda Abelisauridae) from
1047 Late Cretac. Madagascar - 1. *Mem. Soc. Vertebr. Paleontol. - 1. J. Vertebr.*
1048 *Paleontol.* 8, 1–20.
- 1049 Krause, J. M., Ramezani, J., Umazano, A. M., Pol, D., Carballido, J. L., Sterli, J.,
1050 Puerta, P., Cúneo, N. R., Bellosi, E. S. 2020. High-resolution chronostratigraphy

- 1051 of the Cerro Barcino Formation (Patagonia): paleobiologic implications for the
1052 mid-Cretaceous dinosaur-rich fauna of South America. *Gondwana Research*, 80,
1053 33-49.
- 1054 Langer, M.C., Martins, N. de O., Manzig, P.C., Ferreira, G. de S., Marsola, J.C. de A.,
1055 Fortes, E., Lima, R., Sant'ana, L.C.F., Vidal, L. da S., Lorençato, R.H. da S.,
1056 Ezcurra, M.D., 2019. A new desert-dwelling dinosaur (Theropoda, Noosaurinae)
1057 from the Cretaceous of south Brazil. *Sci. Reports* 9, 9379.
- 1058 Makovicky, P.J., Apesteguía, S., Agnolín, F.L., 2005. The earliest dromaeosaurid
1059 theropod from South America. *Nature* 437, 1007–1011.
- 1060 Makovicky, P. J., Apesteguía, S., and Gianechini, F. A. 2012. A new coelurosaurian
1061 theropod from the La Buitrera fossil locality of Río Negro, Argentina. *Fieldiana*
1062 *Life and Earth Sciences*, 2012(5), 90-98.
- 1063 Marsh, O.C., 1881. Principal characters of American Jurassic dinosaurs. *Part V.*
1064 *American Journal of Science*, series 3 (21):417–423.
- 1065 Martinelli, A., and Forasiepi, A. 2004. Late Cretaceous vertebrates from Bajo de Santa
1066 Rosa (Allen Formation), Río Negro province, Argentina, with the description of
1067 a new sauropod dinosaur (Titanosauridae). *Revista del Museo Argentino de*
1068 *Ciencias Naturales Nueva Serie*, 6(2), 257-305.
- 1069 Martinelli, A.G., and Teixeira, V.P.A., 2015. The Late Cretaceous vertebrate record
1070 from the Bauru Group at the Triângulo Mineiro, southeastern Brazil. *Boletín*
1071 *Geológico y Minero de España* 126(1): 129-158.

- 1072 Martínez, R.D., Giménez, O. del V., Rodríguez, J., Bochaty, G., 1986.
1073 *Xenotarsosaurus bonapartei* gen. et. sp. nov. (Carnosauria, Abelisauridae), un
1074 nuevo Theropoda de la Formación Bajo Barreal, Chubut, Argentina, in: 4°
1075 Congreso Argentino de Paleontología y Bioestratigrafía. Actas, pp. 23–31.
- 1076 Martínez, R.D., Novas, F.E., 2006. *Aniksosaurus darwini* gen. et sp. nov., a new
1077 coelurosaurian theropod from the Early Late Cretaceous of Central Patagonia,
1078 Argentina. *Rev. del Mus. Argentino Ciencias Nat. nueva Ser.* 8, 243–259.
- 1079 Martínez, R.D., Lamanna, M.C., Novas, F.E., Ridgely, R.C., Casal, G.A., Martínez,
1080 J.E., Vita, J.R., Witmer, L.M., 2016. A basal lithostrotian titanosaur (Dinosauria:
1081 Sauropoda) with a complete skull: implications for the evolution and
1082 paleobiology of Titanosauria. *Plos One* 11, e0151661.
- 1083 Motta, M. J., Aranciaga Rolando, A. M., Rozadilla, S., Agnolín, F. E., Chimento, N. R.,
1084 Egli, F. B., and Novas, F. E. 2016. New theropod fauna from the upper
1085 cretaceous (Huincul Formation) of Northwestern Patagonia, Argentina. *New*
1086 *Mexico Museum of Natural History and Science Bulletin*, 71, 231-253.
- 1087 Motta, M.J., Agnolín, F.L., Brissón Egli, F., Novas, F.E., 2020. New theropod dinosaur
1088 from the Upper Cretaceous of Patagonia sheds light on the paravian radiation in
1089 Gondwana. *Sci. Nat.* 107, 24.
- 1090 Müller, R. T., Langer, M. C., Bronzati, M., Pacheco, C. P., Cabreira, S. F., and Dias-
1091 Da-Silva, S. 2018. Early evolution of sauropodomorphs: anatomy and
1092 phylogenetic relationships of a remarkably well-preserved dinosaur from the
1093 Upper Triassic of southern Brazil. *Zoological Journal of the Linnean Society*,
1094 184(4), 1187-1248.

- 1095 Novas, F.E., Agnolín, F.L., 2004. *Unquillosaurus ceibali* Powell, a giant maniraptoran
1096 (Dinosauria, Theropoda) from the Late Cretaceous of Argentina. *Rev. del Mus.*
1097 *Argentino Ciencias Nat. nueva Ser.* 6, 61–66.
- 1098 Novas, F.E., de Valais, S., Vickers-Rich, P., Rich, T.H., 2005. A large Cretaceous
1099 theropod from Patagonia, Argentina, and the evolution of carcharodontosaurids.
1100 *Naturwissenschaften* 92, 226–230.
- 1101 Novas, F., Ezcurra, M., Agnolín, F., Pol, D., and Ortiz, R. 2012. New Patagonian
1102 Cretaceous theropod sheds light about the early radiation of Coelurosauria.
1103 *Revista del Museo Argentino de Ciencias Naturales nueva serie*, 14(1).
- 1104 Novas, F. E., Agnolín, F. L., Ezcurra, M. D., Porfiri, J., and Canale, J. I. 2013.
1105 Evolution of the carnivorous dinosaurs during the Cretaceous: the evidence from
1106 Patagonia. *Cretac. Res.*, 45, 174-215.
- 1107 Novas, F.E., Salgado, L., Suárez, M., Agnolín, F.L., Ezcurra, M.D., Chimento, N.R., de
1108 la Cruz, R., Isasi, M.P., Vargas, A.O., Rubilar-Rogers, D., 2015. An enigmatic
1109 plant-eating theropod from the Late Jurassic period of Chile. *Nature* 522, 331–
1110 334.
- 1111 Perea, D., Soto, M., Veroslavsky, G., Daners, G., Mesa, V., Ubilla, M., Martínez, S.A.,
1112 Toriño, P., 2011. Bioestratigrafía y escenarios ambientales del Mesozoico de
1113 Uruguay, in: *Paleontología: Cenários de Vida*. pp. 421–431.
- 1114 Pol, D., Leardi, J.M., 2015. Diversity Patterns of Notosuchia (Crocodyliformes,
1115 Mesoeucrocodylia) During the Cretaceous of Gondwana, in: Fernández, M.S.,
1116 Herrera, Y. (Eds.), 2. *Reptiles Extintos - Volumen En Homenaje a Zulma*
1117 *Gasparini - Publicación Electrónica de La Asociación Paleontológica Argentina*.

- 1118 Porfiri, J.D., Novas, F.E., Calvo, J.O., Agnolín, F.L., Ezcurra, M.D., Cerda, I.A., 2014.
1119 Juvenile specimen of *Megaraptor* (Dinosauria, Theropoda) sheds light about
1120 tyrannosauroid radiation. *Cretac. Res.* 51, 35–55.
- 1121 Porfiri, J.D., Juárez Valieri, R.D., Dos Santos, D.D., Lamanna, M.C., 2018. A new
1122 megaraptoran theropod dinosaur from the Upper Cretaceous Bajo de la Carpa
1123 Formation of northwestern Patagonia. *Cretac. Res.* 89, 302–319.
- 1124 Rauhut, O.W.M., 2004. Provenance and anatomy of *Genyodectes serus*, a large-toothed
1125 ceratosaur (Dinosauria: Theropoda) from Patagonia. *J. Vertebr. Paleontol.* 24,
1126 894–902.
- 1127 Rauhut, O.W.M., 2011. Theropod dinosaurs from the Late Jurassic of Tendaguru
1128 (Tanzania), in: Barrett, P.M., Milner, A.R.C. (Eds.), *Studies on Fossil Tetrapods*
1129 - Special Papers in Palaeontology. pp. 195–239.
- 1130 Rauhut, O. W., and Carrano, M. T. 2016. The theropod dinosaur *Elaphrosaurus*
1131 *bambergi*, from the Late Jurassic of Tendaguru, Tanzania. *Zoological Journal of*
1132 *the Linnean Society*, 178(3), 546-610.
- 1133 Rauhut, O.W.M., Pol, D., 2017. A theropod dinosaur from the Late Jurassic Cañadón
1134 Calcáreo Formation of central Patagonia, and the evolution of the theropod
1135 tarsus. *Ameghiniana* 54, 539–566.
- 1136 Rauhut, O. W., Foth, C., Tischlinger, H., and Norell, M. A. 2012. Exceptionally
1137 preserved juvenile megalosauroid theropod dinosaur with filamentous
1138 integument from the Late Jurassic of Germany. *Proceedings of the National*
1139 *Academy of Sciences*, 109(29), 11746-11751.

- 1140 Rauhut, O. W., Huebner, T. R., and Lanser, K. P. 2016. A new megalosaurid theropod
1141 dinosaur from the late Middle Jurassic (Callovian) of north-western Germany:
1142 Implications for theropod evolution and faunal turnover in the Jurassic.
1143 *Palaeontologia Electronica*, (2).
- 1144 Salgado, L., Canudo Sanagustín, J.I., Garrido, A.C., Ruiz-Omeñaca, J.I., García, R.A.,
1145 de la Fuente, M.S., Barco, J.L., Bollati, R., 2009. Upper Cretaceous vertebrates
1146 from El Anfiteatro area, Río Negro, Patagonia, Argentina. *Cretac. Res.* 30, 767–
1147 784.
- 1148 Sereno, P.C., Wilson, J.A., Conrad, J.L., 2004. New dinosaurs link southern landmasses
1149 in the Mid-Cretaceous. 1. Proc. R. Soc. London, Series B (Biological Sciences)
1150 271, 1325–1330.
- 1151 Simón, M.E., Salgado, L., Calvo, J.O., 2018. A new titanosaur sauropod from the Upper
1152 Cretaceous of Patagonia, Neuquén Province, Argentina. *Ameghiniana* 55, 1–29.
- 1153 Smith, J. B., and Dodson, P. 2003. A proposal for a standard terminology of anatomical
1154 notation and orientation in fossil vertebrate dentitions. *Journal of Vertebrate*
1155 *paleontology*, 23(1), 1-12.
- 1156 Smith, J. B., Vann, D. R., and Dodson, P. 2005. Dental morphology and variation in
1157 theropod dinosaurs: implications for the taxonomic identification of isolated
1158 teeth. *The Anatomical Record Part A: Discoveries in Molecular, Cellular, and*
1159 *Evolutionary Biology: An Official Publication of the American Association of*
1160 *Anatomists*, 285(2), 699-736.
- 1161 Stromer, E., 1931. Wirbeltierreste der Baharije-Stufe (unterstes Cenoman). 10. Ein
1162 Skelett-Rest von *Carcharodontosaurus* nov. gen. Abhandlungen Bayerische

- 1163 Akademie Wissenschafte Atheilung naturwissenschaften Abteilung Neue Folge, 9:
1164 1–23.
- 1165 Veralli, C., and Calvo, J. O. 2004. Dientes de terópodos carcharodontosáuridos del
1166 Turoniano superior-Coniaciano inferior del Neuquén, Patagonia, Argentina.
1167 *Ameghiniana*, 41(4), 587-590.
- 1168 Wang, S., Stiegler, J., Amiot, R., Wang, X., Du, G. H., Clark, J. M., and Xu, X. 2017.
1169 Extreme ontogenetic changes in a ceratosaurian theropod. *Current Biology*,
1170 27(1), 144-148.
- 1171 Young, C. M., Hendrickx, C., Challands, T. J., Foffa, D., Ross, D. A., Butler, I. B., and
1172 Brusatte, S. L. 2019. New theropod dinosaur teeth from the Middle Jurassic of
1173 the Isle of Skye, Scotland. *Scottish Journal of Geology*, 55(1), 7-19.

1174

1175 **FIGURE CAPTIONS**

1176 **FIGURE 1.** a) Schematic map of the Neuquén basin and extension of its Cenozoic
1177 sequences (*sensu* Andreis, 2001) and the Golfo San Jorge basin showing each specimen
1178 occurrence site. b) Stratigraphic column for the Upper Cretaceous of the Neuquén basin,
1179 highlighting the lithological units of occurrence for each one specimen (Modified from
1180 Garrido, 2010), and c) Stratigraphic column for the Upper Cretaceous of the Golfo San
1181 Jorge basin, highlighting the lithological unit of occurrence for the specimen,
1182 respectively.

1183 **FIGURE 2.** Location maps of each specimen according to its occurrence *in situ* and the
1184 geological unit that is inserted, respectively. a) MDPA-Pv 005 (Aguada Pichana),

1185 MUCPv 381, 384, 386, 387 (Morphotypes I) and MUCPv 391 (Morphotype II)
1186 (Futalogno Site); **b**) Endemas-Pv 2 (La Bajada Sector); Endemas-Pv 16 (Parrita Site);
1187 **c**) MACN-Pv-RN 1085 (Cerro Bonaparte); and **d**) UNPSJB-PV 969 (Estancia Ocho
1188 Hermanos).

1189 **FIGURE 3.** MDPA-Pv 005 in **A**, labial; **B**, lingual; **C**, distal; **D**, mesial views; **E**, detail
1190 of marginal undulations; **F**, detail of enamel texture; **G**, distal denticles at the apical
1191 three-fourths of the crown height; **H**, basal; **I**, apical views. **Abbreviations:** **mca**,
1192 mesial carina; **dca**, distal carina; **mun**, marginal undulations; **ent**, enamel texture. Scale
1193 bar equal 1 cm.

1194 **FIGURE 4.** Endemas-Pv 2 in **A**, lingual; **B**, labial; **C**, mesial; **D**, distal views; **E**, detail
1195 of marginal undulations; **F**, basal view. **Abbreviations:** **mca**, mesial carina; **dca**, distal
1196 carina; **mun**, marginal undulations. Scale bar equal 1 cm.

1197 **FIGURE 5.** UNPSJB-PV 969 in **A**, labial; **B**, lingual; **C**, mesial; **D**, distal views.
1198 **Abbreviations:** **mca**, mesial carina; **dca**, distal carina. Scale bar equal 1 cm.

1199 **FIGURE 6.** Morphotype I (**A-I**) and II (**J-N**). MUCPv 381 in **A**, labial; **B**, mesial
1200 views. MUCPv 384 in **C**, lingual; **D**, labial; **E**, distal; **F**, mesial views. MUCPv 386 in
1201 **G**, lingual; **H**, labial views. MUCPv 387 in **I**, labial view. MUCPv 391 in **J**, lingual; **K**,
1202 labial; **L**, mesial; **M**, distal; **N**, apical views. **Abbreviations:** **mca**, mesial carina; **dca**,
1203 distal carina; **mun**, marginal undulations. Scale bar equal 1 cm.

1204 **FIGURE 7.** Endemas-Pv 16 in **A**, labial view; **B**, mesial denticles at the mid-crown; **C**,
1205 distal denticles at the mid-crown; **D**, distal denticles close to the base of crown.
1206 **Abbreviations:** **mca**, mesial carina; **dca**, distal carina. Scale bar equal 1 cm.

1207 **FIGURE 8.** MACN-Pv-RN 1085 in **A**, lingual; **B**, labial; **C**, mesial; **D**, distal views; **E**,
1208 mesial and distal denticles at the mid-crown; **F**, basal view. **Abbreviations:** **mca**,
1209 mesial carina; **dca**, distal carina. Scale bar equal 1 cm.

1210 **FIGURE 9.** Strict consensus tree of 100 most parsimonious trees (CI = 0.196; RI =
1211 0.458; L = 1333) recovered in the cladistic analysis of the dentition-based data matrix
1212 with constrained search and setting the all morphotypes as floating terminals.

1213 **FIGURE 10.** Strict consensus tree of 100 most parsimonious trees (CI = 0.178; RI =
1214 0.346; L = 1458) recovered in the cladistic analysis of the dentition-based data matrix
1215 with an unconstrained search.

1216 **FIGURE 11.** Strict consensus tree of 100 most parsimonious trees (CI = 0.112; RI =
1217 0.05; L = 1433) recovered in the cladistic analysis of the tooth-crown-based data matrix.

1218 **FIGURE 12.** Results of the discriminant analysis performed at the “group”-level on the
1219 whole dataset with personal measurements of C.H. on 400 teeth belonging to 46
1220 theropod taxa and 12 groupings along the first two canonical axes of maximum
1221 discrimination in the dataset (PC1 and PC2 account for 38.19% and 30.88% of the total
1222 variance, respectively).

1223 **FIGURE 13.** Results of the discriminant analysis performed at the “group”-level on the
1224 whole dataset with teeth larger than two centimeters, on 725 teeth belonging to 53
1225 theropod taxa and 13 groupings along the first two canonical axes of maximum
1226 discrimination in the dataset (PC1 47.43% and PC2 27.57% of the total variance,
1227 respectively).

1228

1229 **TABLES**

1230 **TABLE 1.** Measurements of all teeth crowns. Measurements in millimeters, number of
1231 denticles per five mm and crown angle in degrees.

1232

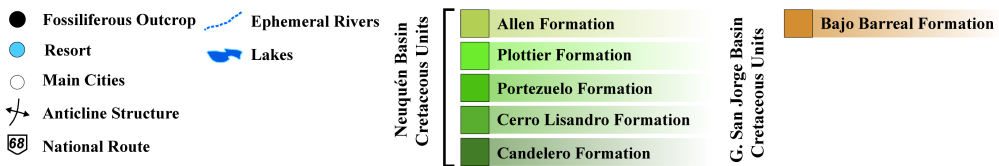
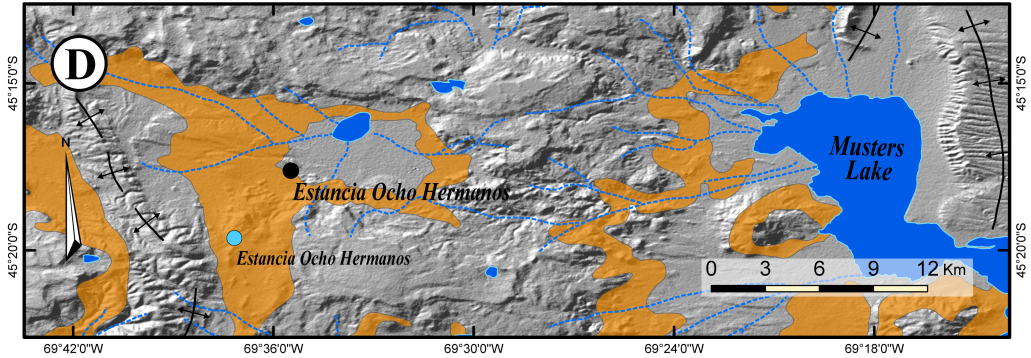
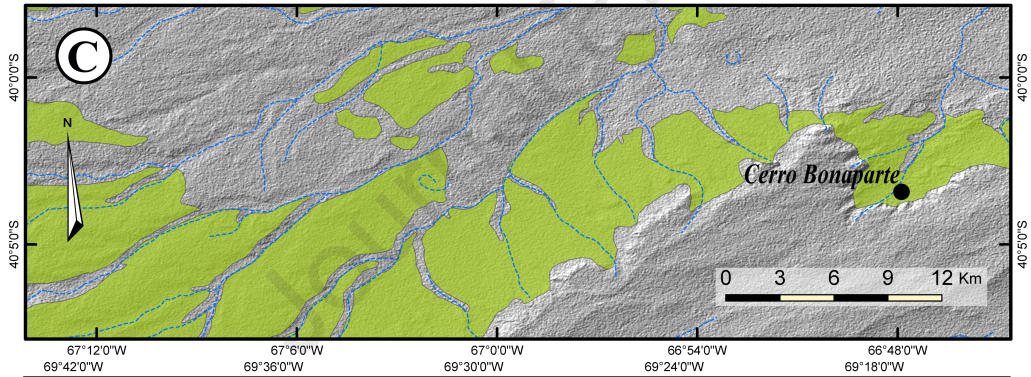
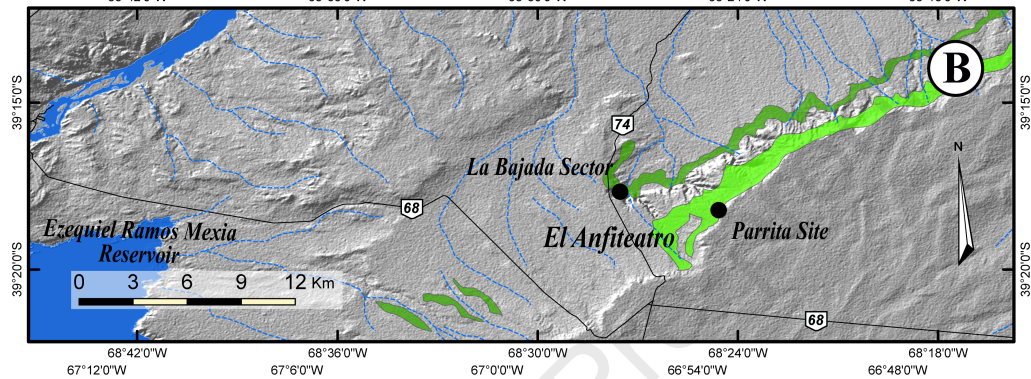
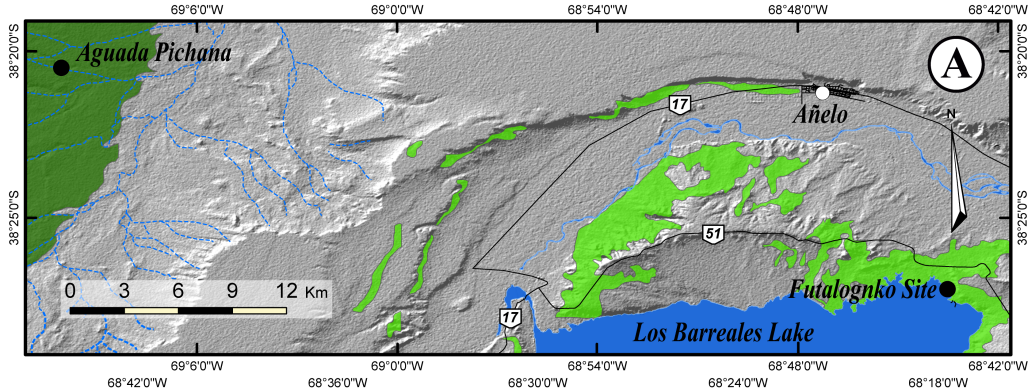
1233 **SUPPLEMENTARY DATA**

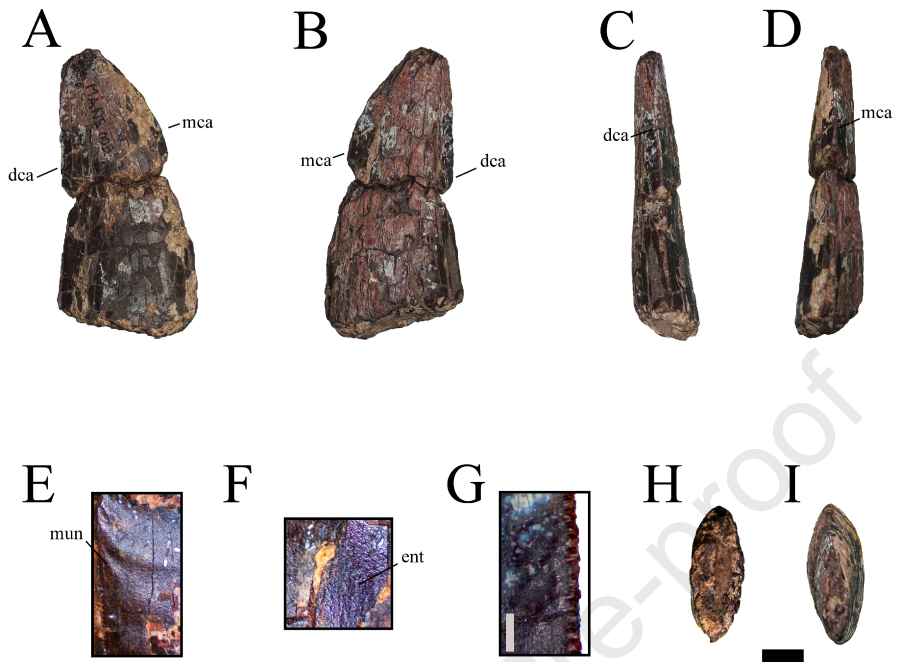
1234

1235

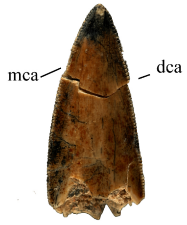
Journal Pre-proof

Specimen	Morphotype	Abbreviation	Anatomical placement	Fuente	CBL	CBW	CH	AL	CBR	CHR	CA	MC	DC	MCL	MCW	MCR	DSDI	
MDPA-Pv 005	Candeleros Morphotype	CdM	Lateral	<i>Observ. Pers.</i>	36.35	16.1	?	?	0.44	?	?	10	15	28	10.6	0.37	1.5	
ENDEMAS-Pv 2	Cerro Lisandro Morphotype	CLM	Mesial	<i>Observ. Pers.</i>	13.5	10.4	31.75	31	0.77	2.35	24.36	12	11	11.2	6.9	0.61	0.9	
UNPSJB-PV 969	Bajo Barreal Morphotype	BBM	Lateral	<i>Observ. Pers.</i>	?	7.4	34.2	34.8	?	2.25	?	13	13	15.7	6.1	0.38	1	
MUCPv386	Portezuelo Morphotype I	PoM1	Lateral	<i>Observ. Pers.</i>	17.2	9.6	?	?	0.55	?	?	11	10	13.2	7.2	0.54	0.9	
MUCPv381				<i>Observ. Pers.</i>	?	?	?	?	?	?	?	?	11	10	10.4	5.6	0.53	0.9
MUCPv384				<i>Observ. Pers.</i>	19.6	9.4	?	?	0.48	?	?	?	11	12	14.5	7.3	0.50	1.09
MUCPv387				<i>Observ. Pers.</i>	16.4	9	?	?	0.54	?	?	?	11	11	12.8	6.5	0.50	1
MUCPv391	Portezuelo Morphotype II	PoM2	Mesial	<i>Observ. Pers.</i>	?	?	?	?	?	?	?	12	11	14.8	8.7	0.58	0.9	
ENDEMAS-Pv 16	Plottier Morphotype	PIM	Lateral	<i>Observ. Pers.</i>	9.5	5	22.8	24.5	0.52	2.4	23.85	15	14	8.1	3.7	0.45	0.9	
MACN-PV RN 1085	Allen Morphotype	AIM	Mesial	<i>Observ. Pers.</i>	?	?	?	?	?	?	?	10	9	10.1	4.9	0.48	0.9	

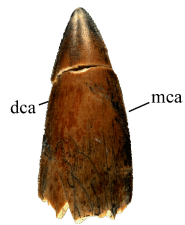




A



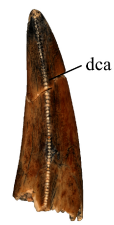
B



C



D



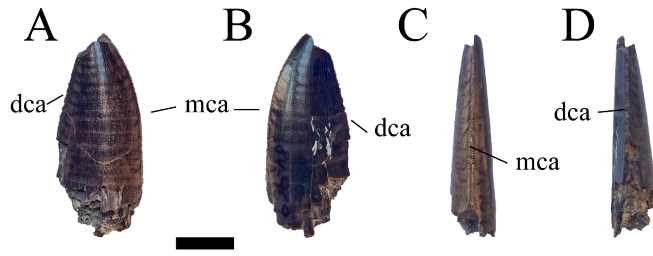
E



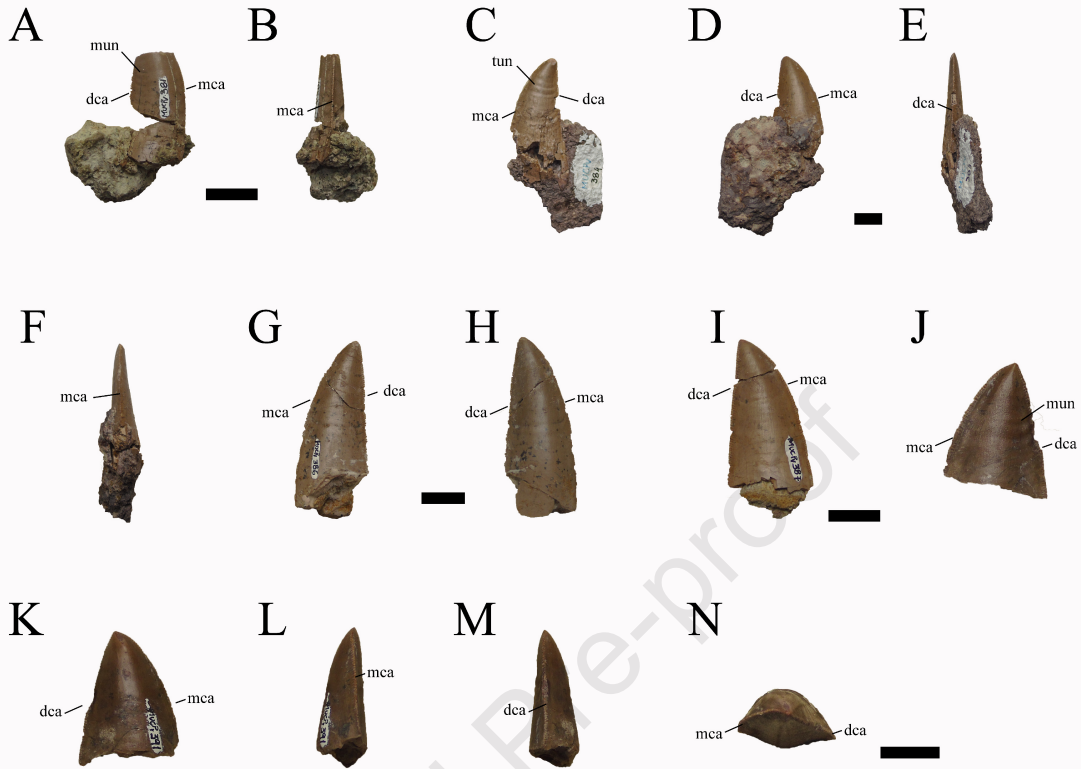
F

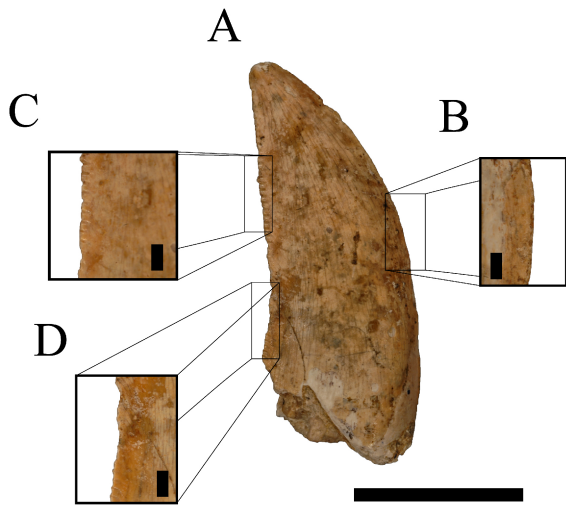


Journal Pre-proof



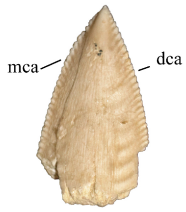
Journal Pre-proof



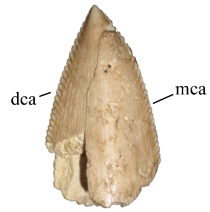


Journal Pre-proof

A



B



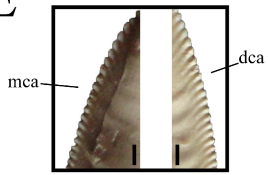
C



D



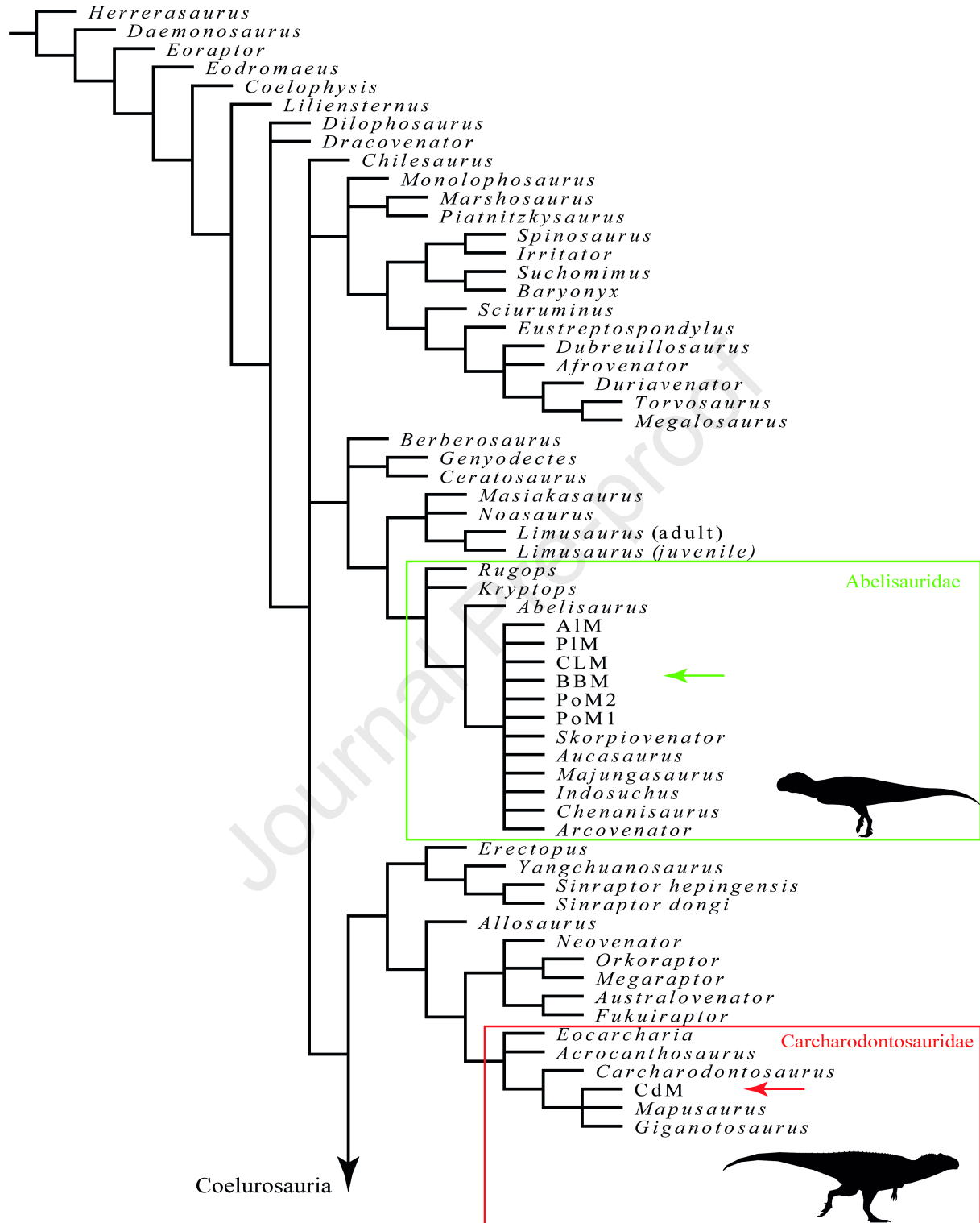
E

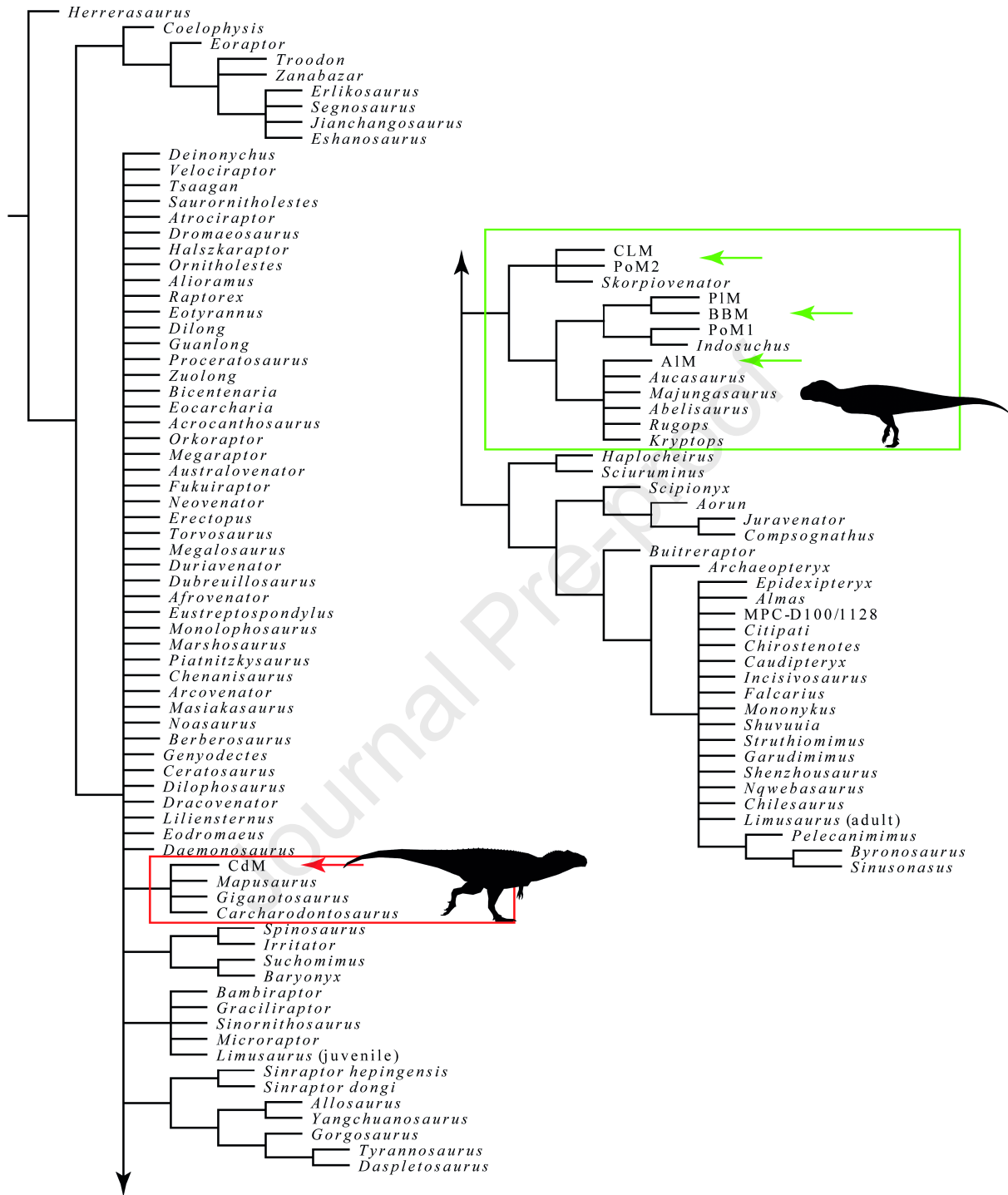


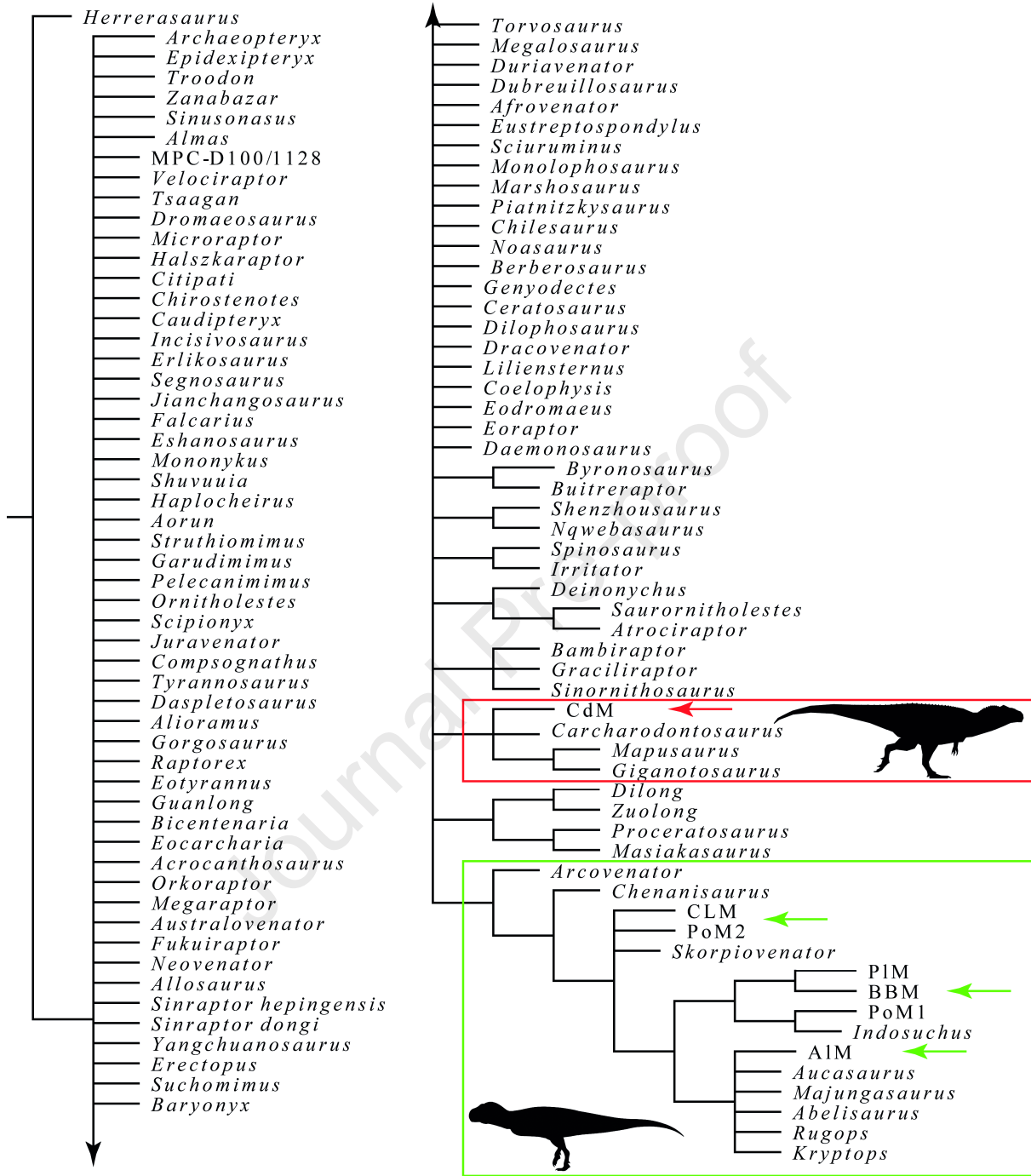
F

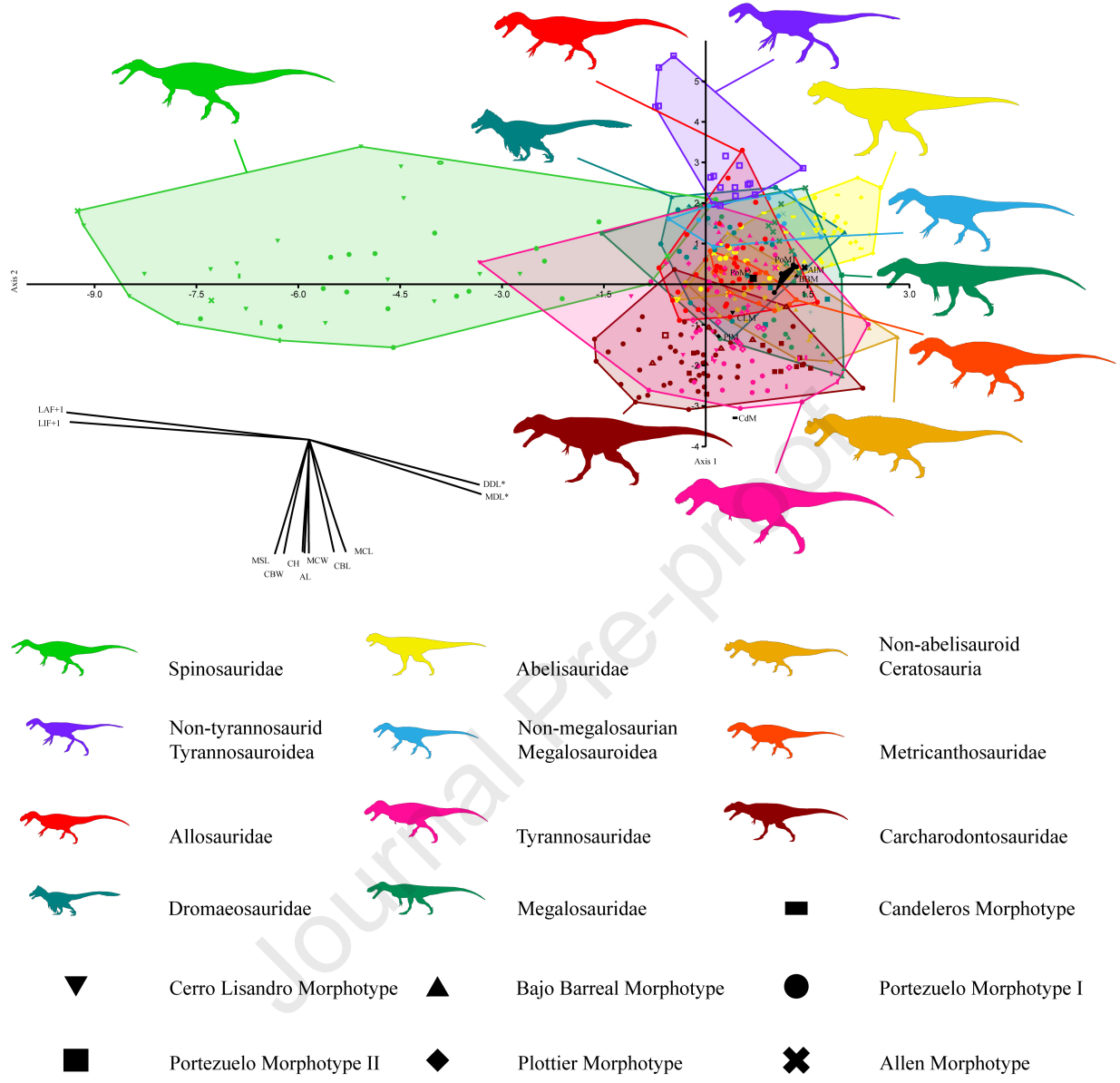


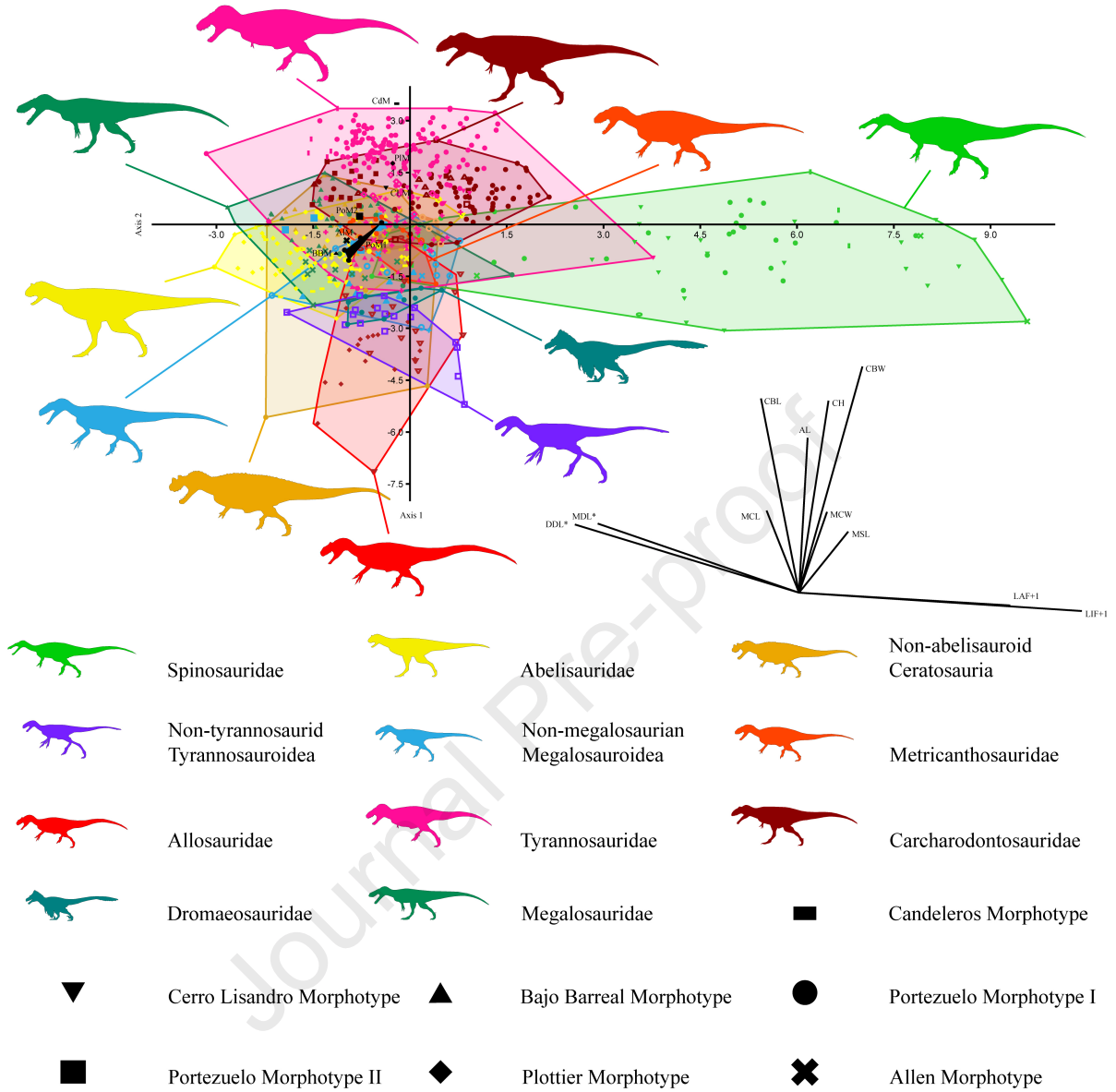
Journal Pre-proof











Declaration of interests

The authors declare that they have no known competing financial interests or personal relationships that could have appeared to influence the work reported in this paper.

The authors declare the following financial interests/personal relationships which may be considered as potential competing interests:

Journal Pre-proof